ON THE SYNTHESIS OF ELEMENTS AT VERY HIGH TEMPERATURES*

ROBERT V. WAGONER, WILLIAM A. FOWLER, AND F. HOYLE
California Institute of Technology, Pasadena, California, and Cambridge University
Received September 1, 1966

ABSTRACT

A detailed calculation of element production in the early stages of a homogeneous and isotropic expanding universe as well as within imploding-exploding supermassive stars has been made. If the recently measured microwave background radiation is due to primeval photons, then significant quantities of only D, He^3, He^4, and Li^7 can be produced in the universal fireball. Reasonable agreement with solar-system abundances for these nuclei is obtained if the present temperature is $3° K$ and if the present density is $\sim 2 \times 10^{-31}$ gm cm^3, corresponding to a deceleration parameter $q_0 \approx 5 \times 10^{-3}$. However, massive stars "bouncing" at temperatures $\sim 10^9 °$ K can convert the universal D and He^3 into C, N, O, Ne, Mg, and some heavier elements in amounts observed in the oldest stars. The mass gaps at $A = 5$ and 8 are bridged by the reactions $He^3(He^4,\gamma)Be^7(He^4,\gamma)C^{11}$. Bounces at higher temperatures bridge the mass gaps through $3 He^4 \to C^{12}$ and mainly produce metals of the iron group, plus a small amount of heavier elements synthesized by a new kind of r-process (rapid neutron capture). It is found that very low abundances of He^4, as recently observed in some stars, can be produced in a universe in which the electron neutrinos are degenerate.

I. INTRODUCTION

In this paper we shall consider the synthesis of elements on short time scales and at very high temperatures. The time scales are typically of the order of 10–10^3 sec, while the temperatures range upward of $10^9 °$ K. These conditions are in marked contrast to the situation in stars, where lower temperatures and longer time scales usually obtain. It will appear that synthesis proceeds differently in many respects, and that abundances, particularly with respect to isotopic composition, are different from those which are produced in stellar nucleosynthesis.

The short time scales of the present paper are applicable to systems in rapid dynamical motion. These include the universe itself, if indeed the universe evolved from a hot, dense state, and also large masses of gas that collapse to such a state and subsequently explode. Our investigation deals with masses upwards of $\sim 10^3 M\odot$.

Nuclear reactions were first applied to the early stages of a Friedmann universe by Alpher, Bethe, and Gamow (1948), and also by Fermi and Turkevich (1950). It was assumed in these investigations that initially all baryons were neutrons, an assumption which placed a severe restriction on the relation between the baryon density ρ_b and temperature. Writing

$$\rho_b = h\, T_9{}^3 \text{ gm cm}^{-3}, \qquad (1)^1$$

where T_9 is in units of $10^9 °$ K, the parameter h had to be set rather precisely ($10^{-6} \gtrsim h \gtrsim 10^{-7}$) in order that hydrogen and helium emerged in approximately equal abundances in the final material. A small change of h was sufficient to make the difference between essentially all hydrogen and essentially all helium.

This situation was changed by Hayashi (1950), who pointed out that at very high temperatures neutrons and protons come into statistical equilibrium through the weak interactions; for example,

$$e^- + p \rightleftarrows n + \nu_e. \qquad (2)$$

[1] It should be noted that eq. (1) only holds exactly if no net energy is being transferred between the electrons and photons due to pair creation and annihilation (see § II).

If none of the electron-leptons (e^-, e^+, ν_e, $\bar{\nu}_e$) is degenerate,[2] then at very high temperatures the mass fractions X_p, X_n satisfy the equation

$$\frac{X_p}{X_n} = e^{(M_n - M_p)c^2/kT} .\qquad (3)$$

It now appeared, both in the calculations of Hayashi and in those of Alpher, Follin, and Herman (1953), that hydrogen and helium emerged in the cooling material in comparable concentrations, provided only that the parameter h in equation (1) was not set too low, $h \gtrsim 10^{-6}$.

It was the hope in these investigations that the synthesis of all elements could be explained in terms of the early history of a Friedmann universe. However, the well-known difficulties at masses 5 and 8 prevented this hope from being realized. Hayashi and Nishida (1956) attempted to evade the difficulties by working at much higher values of the parameter h, i.e., at much higher baryon densities at a given temperature. This enabled the gaps at masses 5 and 8 to be jumped over by the triple-α reaction, $3 \, \text{He}^4 \rightarrow \text{C}^{12}$. But a new difficulty soon emerged. Further nuclear reactions, of the type $\text{C}^{12}(\text{He}^4, \gamma)\text{O}^{16}$ and $\text{C}^{12}(p, \gamma)\text{N}^{13}(\text{He}^4, p)\text{O}^{16}$ produced a buildup toward heavier elements, with the result that effectively all the carbon produced by the triple-α reaction was built into heavy metals in the region of the iron group. This was in disagreement with the observation that C and O are much more abundant than the heavy metals.

Partly for these reasons, and partly because some 10 years ago it was found that stars of different populations differ widely in their metal content, "universal synthesis" was abandoned in favor of stellar nucleosynthesis. The discovery by Merrill (1952) of Tc in S stars served as a conclusive demonstration that the s-process of Burbidge, Burbidge, Fowler, and Hoyle (1957) was operative in stars. Many of the details of the observed abundances of the elements were explained in terms of stellar processes. Yet one major problem remained, the origin of helium. Stars appear to be deficient as producers of the present galactic helium abundance by a factor of as much as 10. This led Hoyle and Tayler (1964) to revive the possibility of a universal synthesis of helium, or of a synthesis in *supermassive objects*[3] preceding the formation of stars in our Galaxy and in other galaxies. Hoyle and Tayler gave a review of the observed helium concentrations in various objects, ranging from about 0.27 by mass in the Sun up to more than 0.40 in some planetary nebulae, and they suggested that the helium concentration may never be low, even in the oldest stars. The observed helium concentrations were found to be explicable for a synthesis at high temperature over a range of the parameter h from 10^{-4} to 10^2. This covered physical cases from a Friedmann universe with $h \approx 10^{-4}$ to isolated massive stars with $M \gtrsim 10^6 \, M\odot$.

Interest in the Friedmann case has been much stimulated by the recent discovery of Penzias and Wilson (1965), that at a wavelength of 7.3 cm the universe has a background temperature of some $3°$ K (see also Dicke, Peebles, Roll, and Wilkinson 1965). A similar value at 3.2 cm has also been found by Roll and Wilkinson (1966), while Field and Hitchcock (1966) and Thaddeus and Clauser (1966) have inferred $\sim 3°$ K at 0.26 cm from the rotational structure of the interstellar absorption bands of CN. Since the universal baryon density cannot average much less than $\sim 3 \times 10^{-31}$ gm cm^{-3} or much more than $\sim 3 \times 10^{-29}$ gm cm^{-3} at the present day, this temperature determination leads to the conclusion that h probably lies in the range 10^{-5}–10^{-3}. Peebles (1966a, b) has reconsidered the Friedmann case with a view to obtaining the solar helium value,

---

[2] Gamow's assumption that initially all baryons were neutrons requires that electron antineutrinos ($\bar{\nu}_e$) be highly degenerate (see § VI).

[3] Throughout the remainder of this paper we will drop the prefix *super* and will refer to these objects as massive stars. However, these stars, with masses $\geq 10^3 M\odot$, are not to be confused with stars with masses in the range 10–100 $M\odot$, which are often referred to as massive stars.

and has found that $h \approx 3 \times 10^{-5}$ does indeed lead to a helium mass fraction of about 0.27.

In this paper it is our aim to do the following:

1. Include in the calculations all significant reactions involving nuclei with atomic weights $A \leq 23$. (In this way we obtain approximate abundances for all individual nuclear species with $A \leq 23$ plus the total abundance for $A \geq 24$. In what follows all nuclei with $A \geq 24$ are designated as $\geq$ Mg.)
2. Consider a wide range of values of h.
3. Consider massive stars with $M \gtrsim 10^3\, M\odot$ as well as the universe.
4. Consider the effects of neutrino degeneracy.

Throughout the paper, we shall make the following assumptions:

1. General relativity (without the cosmological constant) correctly describes the large-scale dynamics of the system.
2. The universe once passed through a phase in which $T \geq 10^{11}$ ° K, while the massive stars reached temperatures $\gtrsim 10^9$ ° K. In an open cosmology, there is no limit to the temperature at an early enough epoch, because in such cosmologies the universe is taken to emerge from a singularity, at which $\rho_b \to \infty$, so that $T \to \infty$. In a closed oscillating cosmology, if such is possible, the temperature at maximum ρ_b must be high enough to disrupt helium into baryons, and effectively to promote "a new deal" so far as the abundances of the elements are concerned. Otherwise there would be a systematic increase in the abundances from cycle to cycle. This is ruled out by observation at least in the case of a large number of cycles in which all matter would be processed to helium or heavier elements.
3. The universe was approximately homogeneous and isotropic within the past light cones of the matter of interest during the element-building epoch. An inhomogeneous universe might be approximated by many massive stars characterized by various values of h. In the massive-star case, we neglect pressure gradients except at the "bounce," and use the dynamics of a sphere of uniform density as a first approximation. A few special cases with longer and shorter time scales than those characteristic of spherical dynamics are treated. We do not require a detailed model for the large-scale dynamics at this stage, since what is of the most importance is merely the time scale in the temperature range at which the nuclear reactions proceed.
4. The electrons are non-degenerate, but not necessarily the neutrinos or antineutrinos.

II. GENERAL PROPERTIES OF THE MATTER

Before considering the reactions among the various nuclei, let us discuss the more general properties of the system. We are concerned with processes occurring in the temperature range $60 \gtrsim T_9 \gtrsim 0.1$. This limits our consideration to the least massive of each family of particles, since $T_9 = 60$ corresponds to an energy of approximately 5 MeV. Therefore there will be present nuclei, protons, neutrons, photons, electrons, positrons, and neutrinos and antineutrinos associated with both electrons and muons.

Since we consider the case $h \approx \rho_b/T_9{}^3 \ll 10^5$, the electrons will be non-degenerate, and so also the baryons, which, however, are also non-relativistic and whose pressure we may neglect. For the most part, we shall assume that $L_{e\nu}$, the ratio of electron lepton number to baryon number satisfies $|L_{e\nu}| \ll 10^3/h$, so that the e-neutrinos will also be non-degenerate. For convenience, we assume the same restriction on the muon lepton number, although the only effect of μ-neutrinos is in the expansion rate. In § VI we consider the effects of neutrino and antineutrino degeneracy.

The formulae we shall use are valid as long as all particles except neutrinos remain in thermal equilibrium with the photons at temperature T. It can easily be shown that photon and particle scattering is sufficient to maintain this condition in the temperature

range of interest. Above $T_9 \approx 100$, the reactions $\pi^{\pm} \rightleftarrows \mu^{\pm} + \nu_{\mu}$ ($\tau \approx 2 \times 10^{-8}$ sec) and $\mu^{\pm} \rightleftarrows e^{\pm} + \nu_e + \nu_{\mu}$ ($\tau \approx 2 \times 10^{-6}$ sec) are fast enough to keep the electron and muon neutrinos in thermal equilibrium if they are non-degenerate. As the temperature drops, however, both types freeze out and expand adiabatically thereafter with the same effective temperature. In the case of massive stars, we assume that the neutrinos escape before undergoing appreciable interaction, so that their density is effectively zero.

In order to specify the dynamical properties of our system, we must know the rate of change of physical distance between particles, as well as the relation between the properties of the medium and this distance measure.

The expansion (+) or contraction (−) rate used is given by

$$\frac{1}{R}\frac{dR}{dt} = \pm \left(\frac{8\pi G}{3}\rho + \frac{\lambda c^2}{3} - k\frac{c^2}{R^2}\right)^{1/2} \approx \pm \left(\frac{8\pi G}{3}\rho\right)^{1/2},$$ (4)

where $R(t)$ is the distance measure, G the gravitational constant, λ the cosmological constant in cm^{-2}, ρ the total mass-energy density in gm cm^{-3}, and $k = -1$ for an open universe, $+1$ for a closed universe, and 0 for a Euclidean universe. In our calculations, $\lambda = 0$. The approximate relations holds in two circumstances:

a) During the high-density ($\rho \gtrsim 10^{-20}$ gm/cm^3) phase of a closed or open, or at any stage in a Euclidean Friedmann universe.

b) Within a spherically symmetric and homogeneous isolated mass having zero kinetic energy upon dispersal to infinity. (In this case, $k = 0$.) Of course, in an actual body there must be a pressure gradient, whose effect we assume negligible, except during a "bounce."

Both of these cases are described by the metric

$$ds^2 = c^2 dt^2 - R^2(t)\left\{\frac{dr^2 + r^2(d\theta^2 + \sin^2\theta \, d\phi^2)}{[1 + (k/4)r^2]^2}\right\},$$ (5)

where r is a comoving radial coordinate.

The second relation needed, the work-energy equation, can be expressed in general as

$$\frac{\partial}{\partial t}(\rho \sqrt{-g}) + \frac{p}{c^2}\frac{\partial}{\partial t}(\sqrt{-g}) = 0$$ (6)

if comoving coordinates and proper time are employed, where p is the total pressure and g is the determinant of the metric. For the metric (5), this becomes

$$\frac{d}{dt}(\rho R^3) + \frac{p}{c^2}\frac{d}{dt}(R^3) = 0.$$ (7)

An additional quantity of interest is q_0, the deceleration parameter corresponding to the present epoch (Sandage 1961). It is related to the present Hubble expansion parameter H_0, the present mass-energy density ρ_0, and the present pressure $p_0 \approx 0$, by the equation

$$q_0 = \left(-\frac{R\ddot{R}}{\dot{R}^2}\right)_0 = \frac{4\pi G}{3H_0^2}\left(\rho_0 + \frac{3p_0}{c^2} - \frac{\lambda c^2}{4\pi G}\right)$$

$$\approx \frac{1}{2}\left(1 - \frac{\lambda c^2}{H_0^2} + \frac{kc^2}{H_0^2 R_0^2}\right) \left.\begin{array}{ll} > \frac{1}{2} & (k = +1) \\ = \frac{1}{2} & (k = 0) \\ = 0 \text{ to } \frac{1}{2} & (k = -1) \\ = -1 \text{ (steady state)}. \end{array}\right\}$$ (8)

Taking $\lambda = 0$, $H_0 = 100$ km (sec-Mpc)$^{-1}$ = $(3.086 \times 10^{17}$ sec)$^{-1}$ = $(0.98 \times 10^{10}$ yr)$^{-1}$ (Sandage 1962) and expressing ρ_0 in gm cm^{-3} and the present temperature T_0 in $^\circ$ K gives

$$q_0 = 2.66 \times 10^{28} \rho_0 = 26.6 \, h T_0{}^3 \rightarrow 718 \, h \text{ for } T_0 = 3^\circ \text{ K} . \tag{9}$$

The thermodynamic relations that we shall need are derived in Appendix A. The main results are summarized in Table 1 for the case of non-degenerate neutrinos.

In Figure 1 are plotted the general properties of the matter in the case of the universe. The same general relations hold approximately within a massive star for all particles except the neutrinos.

TABLE 1

$$\rho_\gamma = 8.42 \, T_9{}^4 \text{ gm cm}^{-3} \qquad\qquad p_\gamma = \tfrac{1}{3} \rho_\gamma c^2 \text{ erg cm}^{-3}$$

$$\rho_\nu = \tfrac{7}{4} \rho_\gamma \left(\frac{T_\nu}{T}\right)^4 \qquad\qquad p_\nu = \tfrac{1}{3} \rho_\nu c^2$$

$$\rho_e = \tfrac{7}{4} \rho_\gamma \, (T_9 \gg 6) \qquad\qquad p_e = \tfrac{1}{3} \rho_e c^2 \, (T_9 \gg 6)$$

$$\rho = \rho_\gamma + \rho_e + \rho_\nu + \rho_b$$

$T \propto R^{-1}$, except during pair creation or annihilation.

$$T_\nu \propto R^{-1} \qquad\qquad T_\nu = T \, (T_9 \gg 6)$$

$$\frac{dT}{dt} = \mp \frac{\rho^{1/2}}{446} \left[\rho_1(T) + \frac{p_1(T)}{c^2} \right] \left[\frac{d\rho_1(T)}{dT} \right]^{-1} ,$$

where $\rho_1(T) = \rho_\gamma + \rho_e$, $p_1(T) = p_\gamma + p_e$,   and t is in seconds .

$$T_9 = 10.4 \, t^{-1/2} \qquad\qquad (T_9 \gg 6)$$

$$\left(\frac{T}{T_\nu}\right) = \left[\frac{2.75 \, (\rho_\gamma + p_\gamma/c^2)}{\rho_1(T) + p_1(T)/c^2} \right]^{1/3} \rightarrow 1.40 \qquad\qquad (T_9 \ll 6) .$$

Using conservation of baryon number and neglecting the effect of energy gain or loss in the nuclear reactions gives the relation

$$\rho_b R^3 = \text{const} , \tag{10}$$

while the baryon pressure is negligible. The evolution of the density must be specified in the calculation. Such a specification will turn out to be equivalent to a choice of the parameter h. It follows that the baryons have negligible effect in equation (7), which may now be written as

$$\frac{1}{R^2} \frac{d}{dR} [R^3 (\rho_\gamma + \rho_e + \rho_\nu)] + \rho_\gamma + \rho_\nu + \frac{3 p_e}{c^2} = 0 . \tag{11}$$

This is the equation of adiabatic expansion. It serves to determine the temperature of the radiation as a function of R. Then equation (4) serves to determine both R and T as functions of the time.

At high temperatures $(T_9 \gtrsim 100)$, all constituents are in thermal equilibrium, so that the neutrino temperature T_ν is the same as the photon temperature T. Since at these temperatures all the terms in equation (11) have the same dependence on temperature, this equation gives $T \propto R^{-1}$.

By the time the temperature has dropped to $T_9 \approx 10$, the neutrinos no longer interact

with the other particles. They are thus "frozen out," and equation (11) separates into two equations,

$$\frac{1}{R^2}\frac{d}{dR}[R^3(\rho_\gamma + \rho_e)] + \rho_\gamma + \frac{3p_e}{c^2} = 0 \tag{12}$$

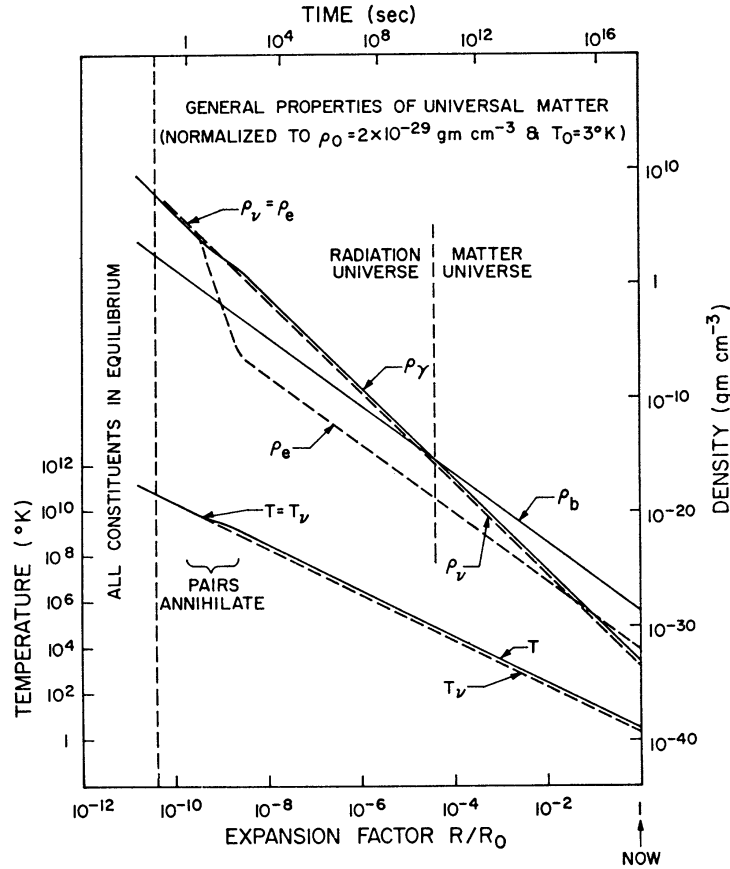$$\frac{1}{R^2}\frac{d}{dR}(R^3\rho_\nu) + \rho_\nu = 0 . \tag{13}$$

Fig. 1.—Densities of baryons, electrons, neutrinos, and photons, as well as photon and neutrino temperatures during the expansion of a homogeneous and isotropic universe from very high temperature. This is a generalized version of Fig. 1 of Dicke *et al.* (1965).

Equation (12) now determines T as a function of R. It will not be a simple relation, since the $e^\pm$ density and pressure are complicated functions of T in the temperature range where they are annihilating into the radiation field. The relations are given in Appendix A. This conversion raises the temperature of the photons relative to the neutrinos. Equation (13) now integrates immediately to give $\rho_\nu \propto R^{-4}$. Since $\rho_\nu \propto T_\nu^4$, T_ν remains proportional to R^{-1}.

As T_9 falls below ~1, the pairs disappear, and equation (12) effectively becomes

$$\frac{1}{R^2}\frac{d}{dR}(R^3\rho_\gamma) + \rho_\gamma = 0 , \tag{14}$$

giving $\rho_\gamma \propto R^{-4}$, so that $T \propto R^{-1}$ again. Since $\rho_b \propto R^{-3}$, we obtain equation (1), defining the parameter h, which is inversely proportional to the entropy of the photons. Prior to

$T_9 \approx 10$, equation (1) holds with an effective value for h equal to the ultimate value multiplied by 2.75.

It should be noted that since $\rho_\nu \propto R^{-4}$, equation (12) actually holds at all temperatures. Then equations (4) and (12) give the relation between temperature and time which is needed to integrate the rate equations. The result is expressed in the equation for dT/dt in Table 1.

III. NUCLEAR REACTIONS AND THEIR RATES

We have considered both the magnitude of the cross-sections and the probable abundance of the various constituents in deciding which reactions are most important in determining the abundances of the various nuclei. Table 2 gives a list of the 144 reactions included, with the corresponding rates. Table 2 also lists the energy released, Q in MeV, in each reaction listed. In the case of positron emission the energy release includes 1.022 MeV from the annihilation of the positron. Subscripts are appended to the rates in those cases where it is necessary to distinguish between various end products. Flow diagrams are presented in Figures 2a and 2b. It is to be noted that in almost all cases both the direct and inverse reactions have been included, although this was not always necessary. Except for the lighter nuclei, the incident particles are protons and alpha-particles.

Except in the case of the neutron, we have included only the free decay of the short-lived β-unstable nuclei. This appears to be a fairly good approximation, since the strong interactions should control the abundances in the region $T_9 \gtrsim 1$ where these weak processes could be important, even though the number density of electrons and neutrinos can be large compared to that of baryons. We have not explicitly included the β decays having long lifetimes, since we simply add the abundance of the unstable nucleus to that of the decay product at the end of the calculation, e.g., $\mathrm{Be}^7 \to \mathrm{Li}^7$.

In describing the abundance of a given nucleus, we use the mass fraction, defined by the relation

$$X_i = \frac{A_i n_i}{\rho_b N_A}, \tag{15}$$

where A_i is the mass number of the ith constituent, n_i, its number density, and N_A, Avogadro's number. The conservation of mass requires $\Sigma_i X_i = 1$.

We wish to construct a differential equation to determine the variation of X_i with time t. To this end we classify the reactions in the following way:

1. Weak interactions (w,β) or photodisintegrations (γ) that either create or destroy nucleus i. The contribution of all such reactions to $(1/A_i)\, dX_i/dt$ can be written formally as $\pm \Sigma_j (X_j/A_j)\, \lambda_k(j)$, in which $\lambda_k(j)$ is the inverse mean lifetime for the reaction between a lepton or photon k with a nucleus j. If $j = i$, i is destroyed by the reaction, and the appropriate term appears with a negative sign, while the opposite is true if $j \neq i$. The specific rate $\lambda_\gamma(j)$ is only a function of temperature.

2. Reactions in which i is destroyed in company with the nucleus j, together with reactions in which nuclei j $(\neq i)$ and k $(\neq i)$ produce i. The effect of all such reactions is given by $\pm \Sigma_{j \geq k} (X_j/A_j)(X_k/A_k)[jk]$, where $[jk] = \rho_b N_A \langle \sigma v \rangle_{jk}$. A term appears with a positive sign if neither j nor k is equal to i; otherwise, with a negative sign. If $j = k \neq i$, the term is multiplied by $\frac{1}{2}$ in the production of i but not in the destruction of j. An appropriate factor, n, must be included if n nuclei of type i are produced in the reaction.

3. Reactions involving three nuclear constituents j, k, ℓ, formally written as $\pm \Sigma_{j \geq k \geq \ell} (X_j/A_j)(X_k/A_k)(X_\ell/A_\ell)[jk\ell]$. A term appears with a positive sign if j, k, and ℓ are all different than i; otherwise with a negative sign. If $j = k \neq \ell \neq i$ the term is multiplied by $\frac{1}{2}$ in the production of i and the destruction of ℓ but not in the destruction of j. If $j = k = \ell \neq i$, the term is multiplied by $\frac{1}{6}$ in the production of i and by $\frac{1}{2}$ in the destruction of j. In practice only one reaction of this type is important, $3\,\mathrm{He}^4 \to \mathrm{C}_{12} + \gamma$.

TABLE 2

REACTIONS INCLUDED AND THEIR RATES (IN SEC^{-1})

(a) *Weak*

		Q(MeV)
(1)	$n + \nu_e \rightleftharpoons p + e^-$	0 7824
(2)	$n + e^+ \rightleftharpoons p + \bar{\nu}_e$	1 804
(3)	$n \rightleftharpoons p + e^- + \bar{\nu}_e$	0 7824

$$\lambda_w(n) = \frac{1}{\tau}\left\{ \int_1^\infty \frac{(\epsilon + q)^2(\epsilon^2 - 1)^{1/2}\epsilon \, d\epsilon}{[1 + e^{-(\epsilon+q)Z_\nu - \phi_\nu}](1 + e^{\epsilon Z})} \right.$$

$$\left. + \int_1^\infty \frac{(\epsilon - q)^2(\epsilon^2 - 1)^{1/2}\epsilon \, d\epsilon}{(1 + e^{-\epsilon Z})[1 + e^{(\epsilon-q)Z_\nu - \phi_\nu}]} \right\}$$

$$\lambda_w(p) = \lambda_w(n)(-q, -\phi_\nu)$$

$$\tau = 1700 \text{ sec}; \quad q = \frac{m_n - m_p}{m_e} = 2.53; \quad \phi_\nu = \Phi_\nu / kT_\nu;$$

$$Z = \frac{m_e c^2}{kT} = \frac{5.93}{T_9}; \quad Z_\nu = \frac{m_e c^2}{kT_\nu} = \frac{5.93}{T_{9\nu}}$$

(4)	$B^8 \rightarrow 2\,He^4 + e^+ + \nu_e$	18 07
	$\lambda_\beta(B^8) = 0.89 \text{ sec}^{-1}$	
(5)	$C^{11} \rightarrow B^{11} + e^+ + \nu_e$	1 981
	$\lambda_\beta(C^{11}) = 5.63 \times 10^{-4}$	
(6)	$N^{12} \rightarrow C^{12} + e^+ + \nu_e$	17 45
	$\lambda_\beta(N^{12}) = 55.4$	
(7)	$N^{13} \rightarrow C^{13} + e^+ + \nu_e$	2 221
	$\lambda_\beta(N^{13}) = 1.15 \times 10^{-3}$	
(8)	$O^{14} \rightarrow N^{14} + e^+ + \nu_e$	5 148
	$\lambda_\beta(O^{14}) = 9.8 \times 10^{-3}$	
(9)	$O^{15} \rightarrow N^{15} + e^+ + \nu_e$	2 761
	$\lambda_\beta(O^{15}) = 5.62 \times 10^{-3}$	
(10)	$F^{17} \rightarrow O^{17} + e^+ + \nu_e$	2 762
	$\lambda_\beta(F^{17}) = 1.05 \times 10^{-2}$	
(11)	$Ne^{18} \rightarrow F^{18} + e^+ + \nu_e$	4 227
	$\lambda_\beta(Ne^{18}) = 0.474$	
(12)	$Ne^{19} \rightarrow F^{19} + e^+ + \nu_e$	3 256
	$\lambda_\beta(Ne^{19}) = 3.85 \times 10^{-2}$	
(13)	$Na^{20} \rightarrow Ne^{20} + e^+ + \nu_e$	15 33
	$\lambda_\beta(Na^{20}) = 1.7$	

10

TABLE 2—*Continued*

Q(MeV)

(14) $\mathrm{Na}^{21} \rightarrow \mathrm{Ne}^{21} + e^{+} + \nu_{e}$ 3 522

$\lambda_{\beta}(\mathrm{Na}^{21}) = 3.0 \times 10^{-2}$

(15) $\mathrm{Mg}^{22} \rightarrow \mathrm{Na}^{22} + e^{+} + \nu_{e}$ 5 04

$\lambda_{\beta}(\mathrm{Mg}^{22}) = 0.178$

(16) $\mathrm{Mg}^{23} \rightarrow \mathrm{Na}^{23} + e^{+} + \nu_{e}$ 4 08

$\lambda_{\beta}(\mathrm{Mg}^{23}) = 5.8 \times 10^{-2}$

(b) Strong and Electromagnetic

(1) $p + n \rightleftarrows \mathrm{D} + \gamma$ 2 225

$[pn] = 2.5 \times 10^{4} \, \rho_{b}$

$\lambda_{\gamma}(\mathrm{D}) = 4.68 \times 10^{9} \, [pn] \, \rho_{b}^{-1} \, T_{9}^{3/2} \exp(-25.82 \, T_{9}^{-1})$

(2) $p + \mathrm{D} \rightleftarrows \mathrm{He}^{3} + \gamma$ 5 494

$[p\mathrm{D}] = 2.23 \times 10^{3} \, \rho_{b} \, T_{9}^{-2/3} \exp(-3.72 \, T_{9}^{-1/3})(1 + 0.112 \, T_{9}^{1/3}$
$\qquad + 3.38 \, T_{9}^{2/3} + 2.65 \, T_{9})$

$\lambda_{\gamma}(\mathrm{He}^{3}) = 1.63 \times 10^{10} \, [p\mathrm{D}] \, \rho_{b}^{-1} \, T_{9}^{3/2} \exp(-63.75 \, T_{9}^{-1})$

(3) $n + \mathrm{D} \rightleftarrows \mathrm{T} + \gamma$ 6 257

$[n\mathrm{D}] = \rho_{b} (75.5 + 1250 \, T_{9})$

$\lambda_{\gamma}(\mathrm{T}) = 1.63 \times 10^{10} \, [n\mathrm{D}] \, \rho_{b}^{-1} \, T_{9}^{3/2} \exp(-72.62 \, T_{9}^{-1})$

(4) $n + \mathrm{He}^{3} \rightleftarrows p + \mathrm{T}$ 0 7638

$[n\mathrm{He}^{3}]_{p} = 7.06 \times 10^{8} \, \rho_{b}$

$[p\mathrm{T}]_{n} = [n\mathrm{He}^{3}]_{p} \exp(-8.864 \, T_{9}^{-1})$

(5) $p + \mathrm{T} \rightleftarrows \mathrm{He}^{4} + \gamma$ 19 81

$[p\mathrm{T}]_{\gamma} = 2.87 \times 10^{4} \, \rho_{b} \, T_{9}^{-2/3} \exp(-3.87 \, T_{9}^{-1/3}) (1 + 0.108 \, T_{9}^{1/3}$
$\qquad + 0.466 \, T_{9}^{2/3} + 0.352 \, T_{9} + 0.300 \, T_{9}^{4/3} + 0.576 \, T_{9}^{5/3})$

$\lambda_{\gamma}(\mathrm{He}^{4})_{p} = 2.59 \times 10^{10} \, [p\mathrm{T}]_{\gamma} \, \rho_{b}^{-1} \, T_{9}^{3/2} \exp(-229.9 \, T_{9}^{-1})$

(6) $n + \mathrm{He}^{3} \rightleftarrows \mathrm{He}^{4} + \gamma$ 20 58

$[n\mathrm{He}^{3}]_{\gamma} = 6.0 \times 10^{3} \, \rho_{b} \, T_{9}$

$\lambda_{\gamma}(\mathrm{He}^{4})_{n} = 2.60 \times 10^{10} \, [n\mathrm{He}^{3}]_{\gamma} \, \rho_{b}^{-1} \, T_{9}^{3/2} \exp(-238.8 \, T_{9}^{-1})$

(7) $\mathrm{D} + \mathrm{D} \rightleftarrows n + \mathrm{He}^{3}$ 3 269

$[\mathrm{DD}]_{n} = 3.9 \times 10^{8} \, \rho_{b} \, T_{9}^{-2/3} \exp(-4.26 \, T_{9}^{-1/3}) (1 + 0.0979 \, T_{9}^{1/3}$
$\qquad + 0.642 \, T_{9}^{2/3} + 0.440 \, T_{9})$

$[n\mathrm{He}^{3}]_{\mathrm{D}} = 1.73 \, [\mathrm{DD}]_{n} \exp(-37.94 \, T_{9}^{-1})$

(8) $\mathrm{D} + \mathrm{D} \rightleftarrows p + \mathrm{T}$ 4.033

$[\mathrm{DD}]_{p} = [\mathrm{DD}]_{n}$

$[p\mathrm{T}]_{\mathrm{D}} = 1.73 \, [\mathrm{DD}]_{p} \exp(-46.80 \, T_{9}^{-1})$

TABLE 2—*Continued*

$Q(\mathrm{MeV})$

(9) $\quad \mathrm{D} + \mathrm{D} \rightleftarrows \mathrm{He}^4 + \gamma$ 23 85

$$[\mathrm{DD}]_\gamma = 24.1\ \rho_b\ T_9^{-2/3}\exp\left(-4.26\ T_9^{-1/3}\right)\left(T_9^{2/3} + 0.685\ T_9\right.$$
$$\left. + 0.152\ T_9^{4/3} + 0.265\ T_9^{5/3}\right)$$
$$\lambda_\gamma(\mathrm{He}^4)_\mathrm{D} = 4.50 \times 10^{10}\ [\mathrm{DD}]_\gamma\ \rho_b^{-1}\ T_9^{3/2}\exp\left(-276.7\ T_9^{-1}\right)$$

(10) $\quad \mathrm{D} + \mathrm{He}^3 \rightleftarrows \mathrm{He}^4 + p$ 18 35

$$[\mathrm{DHe}^3] = 2.60 \times 10^9\ \rho_b\ T_9^{-3/2}\exp\left(-2.99\ T_9^{-1}\right)$$
$$[\mathrm{He}^4 p] = 5.50\ [\mathrm{DHe}^3]\exp\left(-213.0\ T_9^{-1}\right)$$

(11) $\quad \mathrm{D} + \mathrm{T} \rightleftarrows \mathrm{He}^4 + n$ 17 59

$$[\mathrm{DT}] = 1.38 \times 10^9\ \rho_b\ T_9^{-3/2}\exp\left(-0.745\ T_9^{-1}\right)$$
$$[\mathrm{He}^4 n] = 5.50\ [\mathrm{DT}]\exp\left(-204.1\ T_9^{-1}\right)$$

(12) $\quad \mathrm{He}^3 + \mathrm{He}^3 \rightleftarrows \mathrm{He}^4 + p + p$ 12 86

$$[\mathrm{He}^3\mathrm{He}^3] = 1.19 \times 10^{10}\ \rho_b\ T_9^{-2/3}\exp\left(-12.25\ T_9^{-1/3}\right)(1 + 0.0340\ T_9^{1/3})$$
$$[\mathrm{He}^4 pp] = 3.37 \times 10^{-10}\ [\mathrm{He}^3\mathrm{He}^3]\ \rho_b\ T_9^{-3/2}\exp\left(-149.2\ T_9^{-1}\right)$$

(13) $\quad \mathrm{T} + \mathrm{T} \rightleftarrows \mathrm{He}^4 + n + n$ 11 33

$$[\mathrm{TT}] = 1.10 \times 10^9\ \rho_b\ T_9^{-2/3}\exp\left(-4.87\ T_9^{-1/3}\right)(1 + 0.0857\ T_9^{1/3})$$
$$[\mathrm{He}^4 nn] = 3.37 \times 10^{-10}\ [\mathrm{TT}]\ \rho_b\ T_9^{-3/2}\exp\left(-131.5\ T_9^{-1}\right)$$

(14) $\quad \mathrm{He}^3 + \mathrm{T} \rightleftarrows \mathrm{He}^4 + p + n$ 12 10

$$[\mathrm{He}^3\mathrm{T}]_{pn} = 5.60 \times 10^9\ \rho_b\ T_9^{-2/3}\exp\left(-7.72\ T_9^{-1/3}\right)(1 + 0.0540\ T_9^{1/3})$$
$$[\mathrm{He}^4 pn] = 3.37 \times 10^{-10}\ [\mathrm{He}^3\mathrm{T}]_{pn}\ \rho_b\ T_9^{-3/2}\exp\left(-140.4\ T_9^{-1}\right)$$

(15) $\quad \mathrm{He}^3 + \mathrm{T} \rightleftarrows \mathrm{He}^4 + \mathrm{D}$ 14 32

$$[\mathrm{He}^3\mathrm{T}]_\mathrm{D} = 3.88 \times 10^9\ \rho_b\ T_9^{-2/3}\exp\left(-7.72\ T_9^{-1/3}\right)(1 + 0.0540\ T_9^{1/3})$$
$$[\mathrm{He}^4\mathrm{D}] = 1.59\ [\mathrm{He}^3\mathrm{T}]_\mathrm{D}\exp\left(-166.2\ T_9^{-1}\right)$$

(16) $\quad \mathrm{He}^3 + \mathrm{He}^4 \rightleftarrows \mathrm{Be}^7 + \gamma$ 1 587

$$[\mathrm{He}^3\mathrm{He}^4] = 4.8 \times 10^6\ \rho_b\ T_9^{-2/3}\exp\left(-12.8\ T_9^{-1/3}\right)(1 + 0.0326\ T_9^{1/3}$$
$$- 0.219\ T_9^{2/3} - 0.0499\ T_9 + 0.0258\ T_9^{4/3} + 0.0150\ T_9^{5/3})$$
$$\lambda_\gamma(\mathrm{Be}^7) = 1.12 \times 10^{10}\ [\mathrm{He}^3\mathrm{He}^4]\ \rho_b^{-1}\ T_9^{3/2}\exp\left(-18.42\ T_9^{-1}\right)$$

(17) $\quad \mathrm{T} + \mathrm{He}^4 \rightleftarrows \mathrm{Li}^7 + \gamma$ 2 467

$$[\mathrm{THe}^4] = 5.28 \times 10^5\ \rho_b\ T_9^{-2/3}\exp\left(-8.08\ T_9^{-1/3}\right)(1 + 0.0516\ T_9^{1/3})$$
$$\lambda_\gamma(\mathrm{Li}^7) = 1.12 \times 10^{10}\ [\mathrm{THe}^4]\ \rho_b^{-1}\ T_9^{3/2}\exp\left(-28.63\ T_9^{-1}\right)$$

(18) $\quad n + \mathrm{Be}^7 \rightleftarrows p + \mathrm{Li}^7$ 1 643

$$[n\mathrm{Be}^7]_p = 6.74 \times 10^9\ \rho_b$$
$$[p\mathrm{Li}^7]_n = [n\mathrm{Be}^7]_p\exp\left(-19.07\ T_9^{-1}\right)$$

12

TABLE 2—*Continued*

Q(MeV)

(19) $p + Be^7 \rightleftarrows B^8 + \gamma$ 0 1348

$$[pBe^7] = 5.19 \times 10^5 \, \rho_b \, T_9^{-2/3} \exp\left(-10.26 \, T_9^{-1/3}\right)$$
$$(1 + 0.0407 \, T_9^{1/3}) \, [1 - \exp\left(-1.564 \, T_9^{-1}\right)]^{-1}$$
$$\lambda_\gamma(B^8) = 1.31 \times 10^{10} \, [pBe^7] \, \rho_b^{-1} \, T_9^{3/2} \exp\left(-1.564 \, T_9^{-1}\right)$$

(20) $p + Li^7 \rightleftarrows He^4 + He^4$ 17 35

$$[pLi^7]_{He^4} = 1.42 \times 10^9 \, \rho_b \, T_9^{-2/3} \exp\left(-8.47 \, T_9^{-1/3}\right)(1 + 0.0493 \, T_9^{1/3})$$
$$[He^4 He^4]_p = 4.64 \, [pLi^7]_{He^4} \exp\left(-201.3 \, T_9^{-1}\right)$$

(21) $n + Be^7 \rightleftarrows He^4 + He^4$ 18 99

$$[nBe^7]_{He^4} = 1.2 \times 10^7 \, \rho_b \, T_9$$
$$[He^4 He^4]_n = 4.64 \, [nBe^7]_{He^4} \exp\left(-220.4 \, T_9^{-1}\right)$$

(22) $p + B^{10} \rightleftarrows He^4 + Be^7$ 1.148

$$[pB^{10}] = 1.10 \times 10^{11} \, \rho_b \, [T_9^{-2/3} \exp\left(-12.04 \, T_9^{-1/3}\right) + 3.28 \times 10^{-2}$$
$$T_9^{-3/2} \exp\left(-12.35 \, T_9^{-1}\right) + 5.08 \times 10^{-2} \, T_9^{-3/2} \exp\left(-16.18 \, T_9^{-1}\right)]$$
$$[He^4 Be^7]_p = 0.749 \, [pB^{10}] \exp\left(-13.32 \, T_9^{-1}\right)$$

(23) $n + B^{10} \rightleftarrows He^4 + Li^7$ 2 791

$$[nB^{10}] = 5.08 \times 10^8 \, \rho_b$$
$$[He^4 Li^7] = 0.749 \, [nB^{10}] \exp\left(-32.39 \, T_9^{-1}\right)$$

(24) $He^4 + Be^7 \rightleftarrows C^{11} + \gamma$ 7 545

$$[He^4 Be^7]_\gamma = 5.7 \times 10^3 \, \rho_b \, T_9^{-3/2} \exp\left(-6.44 \, T_9^{-1}\right)$$
$$\lambda_\gamma(C^{11}) = 4.06 \times 10^{10} \, [He^4 Be^7]_\gamma \, \rho_b^{-1} \, T_9^{3/2} \exp\left(-87.56 \, T_9^{-1}\right)$$

(25) $He^4 + He^4 + He^4 \rightleftarrows C^{12} + \gamma, \; \gamma \; \text{or} \; e^+, \, e^-$ 7 274

$$[He^4 He^4 He^4] = 1.80 \times 10^{-8} \, \rho_b^2 \, T_9^{-3} \, [\exp\left(-4.32 \, T_9^{-1}\right)$$
$$+ 30.3 \exp\left(-27.4 \, T_9^{-1}\right)]$$
$$\lambda_\gamma(C^{12}) = 2.05 \times 10^{20} \, [He^4 He^4 He^4] \, \rho_b^{-2} \, T_9^3 \exp\left(-84.42 \, T_9^{-1}\right)$$

(26) $p + B^{11} \rightarrow He^4 + He^4 + He^4$ 8 682

$$[pB^{11}] = 3.97 \times 10^5 \, \rho_b \, T_9^{-3/2} \, [\exp\left(-1.74 \, T_9^{-1}\right)$$
$$+ 1.96 \times 10^4 \exp\left(-7.18 \, T_9^{-1}\right)]$$

(27) $p + C^{11} \rightleftarrows N^{12} + \gamma$ 0 573

$$[pC^{11}] = 1.06 \times 10^5 \, \rho_b \, T_9^{-3/2} \exp\left(-5.7 \, T_9^{-1}\right) + 2.05 \times 10^7 \, \rho_b \, T_9^{-2/3}$$
$$\exp\left(-13.7 \, T_9^{-1/3}\right) (1 + 3.04 \times 10^{-2} \, T_9^{1/3} + 1.19 \, T_9^{2/3} + 0.254 \, T_9)$$
$$\lambda_\gamma(N^{12}) = 2.36 \times 10^{10} \, [pC^{11}] \, \rho_b^{-1} \, T_9^{3/2} \exp\left(-6.65 \, T_9^{-1}\right)$$

(28) $He^4 + C^{11} \rightleftarrows p + N^{14}$ 2 920

$$[He^4 C^{11}] = 2.2 \times 10^{16} \, \rho_b \, T_9^{-2/3} \exp\left(-31.9 \, T_9^{-1/3}\right)$$
$$[pN^{14}]_{He^4} = 3.71 \, [He^4 C^{11}] \exp\left(-33.89 \, T_9^{-1}\right)$$

13

TABLE 2—*Continued*

Q(MeV)

(29) $p + C^{12} \rightleftharpoons N^{13} + \gamma$ 1 943

$$[pC^{12}] = 1.06 \times 10^5 \, \rho_b \, T_9^{-3/2} \exp(-4.92 \, T_9^{-1}) + 2.05 \times 10^7 \, \rho_b \, T_9^{-2/3}$$

$$\exp(-13.7 \, T_9^{-1/3})(1 + 3.04 \times 10^{-2} \, T_9^{1/3} + 1.19 \, T_9^{2/3} + 0.254 \, T_9)$$

$$\lambda_\gamma(N^{13}) = 8.87 \times 10^9 \, [pC^{12}] \, \rho_b^{-1} \, T_9^{3/2} \exp(-22.55 \, T_9^{-1})$$

(30) $He^4 + C^{12} \rightleftharpoons O^{16} + \gamma$ 7 161

$$[He^4C^{12}]_\gamma = 2.34 \times 10^8 \, \rho_b \, T_9^{-2} \exp(-32.2 \, T_9^{-1/3})$$

$$\lambda_\gamma(O^{16})_{He^4} = 5.20 \times 10^{10} \, [He^4C^{12}]_\gamma \, \rho_b^{-1} \, T_9^{3/2} \exp(-83.11 \, T_9^{-1})$$

(31) $He^4 + N^{12} \rightleftharpoons p + O^{15}$ 9 641

$$[He^4N^{12}] = 1.2 \times 10^{17} \, \rho_b \, T_9^{-2/3} \exp(-35.6 \, T_9^{-1/3})$$

$$[pO^{15}] = 4.29 \, [He^4N^{12}] \exp(-111.9 \, T_9^{-1})$$

(32) $He^4 + C^{13} \rightleftharpoons n + O^{16}$ 2 215

$$[He^4C^{13}] = 1.2 \times 10^{16} \, \rho_b \, T_9^{-2/3} \exp(-32.3 \, T_9^{-1/3})$$

$$[nO^{16}] = 5.87 \, [He^4C^{13}] \exp(-25.72 \, T_9^{-1})$$

(33) $p + C^{13} \rightleftharpoons N^{14} + \gamma$ 7 549

$$[pC^{13}] = 1.34 \times 10^6 \, \rho_b \, T_9^{-3/2} \exp(-5.97 \, T_9^{-1}) + 8.04 \times 10^7 \, \rho_b \, T_9^{-2/3}$$

$$\exp(-13.7 \, T_9^{-1/3})(1 + 0.0304 \, T_9^{1/3} + 0.958 \, T_9^{2/3} + 0.204 \, T_9)$$

$$\lambda_\gamma(N^{14}) = 1.20 \times 10^{10} \, [pC^{13}] \, \rho_b^{-1} \, T_9^{3/2} \exp(-87.61 \, T_9^{-1})$$

(34) $p + N^{14} \rightleftharpoons O^{15} + \gamma$ 7 292

$$[pN^{14}]_\gamma = 4.2 \times 10^7 \, \rho_b \, T_9^{-2/3} \exp(-15.2 \, T_9^{-1/3}) + 2.2 \times 10^3 \, \rho_b \, T_9^{-3/2}$$

$$\exp(-3.01 \, T_9^{-1})$$

$$\lambda_\gamma(O^{15}) = 2.73 \times 10^{10} \, [pN^{14}]_\gamma \, \rho_b^{-1} \, T_9^{3/2} \exp(-84.62 \, T_9^{-1})$$

(35) $He^4 + N^{13} \rightleftharpoons p + O^{16}$ 5 218

$$[He^4N^{13}] = 1.5 \times 10^{17} \, \rho_b \, T_9^{-2/3} \exp(-35.9 \, T_9^{-1/3})$$

$$[pO^{16}]_{He^4} = 5.86 \, [He^4N^{13}] \exp(-60.55 \, T_9^{-1})$$

(36) $p + N^{13} \rightleftharpoons O^{14} + \gamma$ 4 626

$$[pN^{13}] = 4.2 \times 10^7 \, \rho_b \, T_9^{-2/3} \exp(-15.2 \, T_9^{-1/3})$$

$$\lambda_\gamma(O^{14}) = 3.59 \times 10^{10} \, [pN^{13}] \, \rho_b^{-1} \, T_9^{3/2} \exp(-53.68 \, T_9^{-1})$$

(37) $He^4 + O^{14} \rightleftharpoons p + F^{17}$ 1 192

$$[He^4O^{14}] = 7.2 \times 10^{17} \, \rho_b \, T_9^{-2/3} \exp(-39.3 \, T_9^{-1/3})$$

$$[pF^{17}]_{He^4} = 0.500 \, [He^4O^{14}] \exp(-13.81 \, T_9^{-1})$$

(38) $p + N^{15} \rightleftharpoons He^4 + C^{12}$ 4 965

$$[pN^{15}] = 8.17 \times 10^{11} \, \rho_b \, T_9^{-2/3} \exp(-15.2 \, T_9^{-1/3})(1 + 0.0274 \, T_9^{1/3}$$

$$+ 6.72 \, T_9^{2/3} + 1.29 \, T_9) + 1.27 \times 10^8 \, \rho_b \, T_9^{-3/2} \exp(-3.68 \, T_9^{-1})$$

$$[He^4C^{12}]_p = 0.700 \, [pN^{15}] \exp(-57.62 \, T_9^{-1})$$

14

TABLE 2—*Continued*

$Q(\text{MeV})$

(39) $\text{He}^4 + \text{O}^{15} \rightleftarrows \text{Ne}^{19} + \gamma$ 3 533

$$[\text{He}^4\text{O}^{15}]_\gamma = 1.9 \times 10^3 \, \rho_b \, T_9^{1/2} \exp(-12.1 \, T_9^{-1})$$

$$\lambda_\gamma(\text{Ne}^{19}) = 5.6 \times 10^{10} \, [\text{He}^4\text{O}^{15}]_\gamma \, \rho_b^{-1} \, T_9^{3/2} \exp(-41.00 \, T_9^{-1})$$

(40) $\text{He}^4 + \text{O}^{16} \rightleftarrows \text{Ne}^{20} + \gamma$ 4 730

$$[\text{He}^4\text{O}^{16}]_\gamma = 38 \, \rho_b \, T_9^{-3/2} \, [\exp(-10.35 \, T_9^{-1}) + 8.4 \exp(-12.2 \, T_9^{-1})$$

$$+ \, 23.4 \exp(-23.1 \, T_9^{-1})]$$

$$\lambda_\gamma(\text{Ne}^{20}) = 5.71 \times 10^{10} \, [\text{He}^4\text{O}^{16}]_\gamma \, \rho_b^{-1} \, T_9^{3/2} \exp(-54.89 \, T_9^{-1})$$

(41) $p + \text{O}^{16} \rightleftarrows \text{F}^{17} + \gamma$ 0 598

$$[p\text{O}^{16}]_\gamma = 1.69 \times 10^8 \, \rho_b \, T_9^{-2/3} \exp(-16.7 \, T_9^{-1/3})$$

$$\lambda_\gamma(\text{F}^{17}) = 3.06 \times 10^9 \, [p\text{O}^{16}]_\gamma \, \rho_b^{-1} \, T_9^{3/2} \exp(-6.94 \, T_9^{-1})$$

(42) $p + \text{O}^{17} \rightleftarrows \text{He}^4 + \text{N}^{14}$ 1 193

$$[p\text{O}^{17}] = 6.5 \times 10^{12} \, \rho_b \, T_9^{-2/3} \exp(-16.6 \, T_9^{-1/3})$$

$$[\text{He}^4\text{N}^{14}] = 0.672 \, [p\text{O}^{17}] \exp(-13.84 \, T_9^{-1})$$

(43) $p + \text{F}^{17} \rightleftarrows \text{Ne}^{18} + \gamma$ 3 922

$$[p\text{F}^{17}]_\gamma = 6.6 \times 10^3 \, \rho_b \, T_9^{1/2} \exp(-7.70 \, T_9^{-1})$$

$$\lambda_\gamma(\text{Ne}^{18}) = 1.10 \times 10^{11} \, [p\text{F}^{17}]_\gamma \, \rho_b^{-1} \, T_9^{3/2} \exp(-45.51 \, T_9^{-1})$$

(44) $\text{He}^4 + \text{F}^{17} \rightleftarrows p + \text{Ne}^{20}$ 4 129

$$[\text{He}^4\text{F}^{17}] = 4.9 \times 10^{18} \, \rho_b \, T_9^{-2/3} \exp(-43.0 \, T_9^{-1/3})$$

$$[p\text{Ne}^{20}]_{\text{He}^4} = 18.8 \, [\text{He}^4\text{F}^{17}] \exp(-47.92 \, T_9^{-1})$$

(45) $p + \text{F}^{19} \rightleftarrows \text{He}^4 + \text{O}^{16}$ 8 115

$$[p\text{F}^{19}] = 4.2 \times 10^{10} \, \rho_b \, T_9^{-2/3} \exp(-12.1 \, T_9^{-1/3})$$

$$[\text{He}^4\text{O}^{16}]_p = 0.645 \, [p\text{F}^{19}] \exp(-94.17 \, T_9^{-1})$$

(46) $\text{He}^4 + \text{Ne}^{18} \rightleftarrows p + \text{Na}^{21}$ 2 640

$$[\text{He}^4\text{Ne}^{18}] = 2.5 \times 10^{19} \, \rho_b \, T_9^{-2/3} \exp(-46.5 \, T_9^{-1/3})$$

$$[p\text{Na}^{21}]_{\text{He}^4} = 0.795 \, [\text{He}^4\text{Ne}^{18}] \exp(-30.64 \, T_9^{-1})$$

(47) $p + \text{F}^{18} \rightleftarrows \text{He}^4 + \text{O}^{15}$ 2 877

$$[p\text{F}^{18}] = [p\text{F}^{19}]$$

$$[\text{He}^4\text{O}^{15}]_p = 0.493 \, [p\text{F}^{18}] \exp(-33.39 \, T_9^{-1})$$

(48) $\text{He}^4 + \text{Ne}^{19} \rightleftarrows p + \text{Na}^{22}$ 2 070

$$[\text{He}^4\text{Ne}^{19}] = [\text{He}^4\text{Ne}^{18}]$$

$$[p\text{Na}^{22}]_{\text{He}^4} = 0.920 \, [\text{He}^4\text{Ne}^{19}] \exp(-24.02 \, T_9^{-1})$$

(49) $p + \text{Ne}^{19} \rightleftarrows \text{Na}^{20} + \gamma$ 0.761

$$[p\text{Ne}^{19}] = 890 \, \rho_b \, T_9^{1/2} \exp(-8.40 \, T_9^{-1})$$

$$\lambda_\gamma(\text{Na}^{20}) = 3.7 \times 10^{10} \, [p\text{Ne}^{19}] \, \rho_b^{-1} \, T_9^{3/2} \exp(-8.83 \, T_9^{-1})$$

TABLE 2—*Continued*

		$Q(\text{MeV})$
(50)	$p + \text{Ne}^{20} \rightleftarrows \text{Na}^{21} + \gamma$	2 432

$$[p\text{Ne}^{20}]_\gamma = 1.4 \times 10^5 \, \rho_b \, T_9^{-3/2} \exp\left(-4.17 \, T_9^{-1}\right)$$

$$\lambda_\gamma(\text{Na}^{21}) = 4.65 \times 10^9 \, [p\text{Ne}^{20}]_\gamma \, \rho_b^{-1} \, T_9^{3/2} \exp\left(-28.22 \, T_9^{-1}\right)$$

(51) $\quad \text{He}^4 + \text{Ne}^{20} \rightleftarrows \text{Mg}^{24} + \gamma$ $\hspace{4cm}$ 9 317

$$[\text{He}^4\text{Ne}^{20}]_\gamma = 3.35 \times 10^4 \, \rho_b \, T_9^{1/2} \exp\left(-15.69 \, T_9^{-1}\right)$$

$$\lambda_\gamma(\text{Mg}^{24}) = 6.09 \times 10^{10} \, [\text{He}^4\text{Ne}^{20}]_\gamma \, \rho_b^{-1} \, T_9^{3/2} \exp\left(-108.1 \, T_9^{-1}\right)$$

(52) $\quad \text{He}^4 + \text{Na}^{20} \rightleftarrows p + \text{Mg}^{23}$ $\hspace{4cm}$ 8 888

$$[\text{He}^4\text{Na}^{20}] = 1.0 \times 10^{20} \, \rho_b \, T_9^{-2/3} \exp\left(-49.9 \, T_9^{-1/3}\right)$$

$$[p\text{Mg}^{23}]_{\text{He}^4} = 0.813 \, [\text{He}^4\text{Na}^{20}] \exp\left(-103.1 \, T_9^{-1}\right)$$

(53) $\quad p + \text{Ne}^{21} \rightleftarrows \text{Na}^{22} + \gamma$ $\hspace{4cm}$ 6 741

$$[p\text{Ne}^{21}] = 4.0 \times 10^4 \, \rho_b \, T_9^{1/2} \exp\left(-8.23 \, T_9^{-1}\right)$$

$$\lambda_\gamma(\text{Na}^{22}) = 1.07 \times 10^{10} \, [p\text{Ne}^{21}] \, \rho_b^{-1} \, T_9^{3/2} \exp\left(-78.23 \, T_9^{-1}\right)$$

(54) $\quad \text{He}^4 + \text{Ne}^{21} \rightleftarrows n + \text{Mg}^{24}$ $\hspace{4cm}$ 2 557

$$[\text{He}^4\text{Ne}^{21}] = [\text{He}^4\text{Ne}^{18}]$$

$$[n\text{Mg}^{24}] = 13.1 \, [\text{He}^4\text{Ne}^{21}] \exp\left(-29.67 \, T_9^{-1}\right)$$

(55) $\quad p + \text{Na}^{21} \rightleftarrows \text{Mg}^{22} + \gamma$ $\hspace{4cm}$ 5 244

$$[p\text{Na}^{21}]_\gamma = 3.0 \times 10^3 \, \rho_b \, T_9^{1/2} \exp\left(-9.06 \, T_9^{-1}\right)$$

$$\lambda_\gamma(\text{Mg}^{22}) = 7.47 \times 10^{10} \, [p\text{Na}^{21}]_\gamma \, \rho_b^{-1} \, T_9^{3/2} \exp\left(-60.86 \, T_9^{-1}\right)$$

(56) $\quad \text{He}^4 + \text{Na}^{21} \rightleftarrows p + \text{Mg}^{24}$ $\hspace{4cm}$ 6 884

$$[\text{He}^4\text{Na}^{21}] = [\text{He}^4\text{Na}^{20}]$$

$$[p\text{Mg}^{24}] = 13.1 \, [\text{He}^4\text{Na}^{21}] \exp\left(-79.89 \, T_9^{-1}\right)$$

(57) $\quad p + \text{Na}^{22} \rightleftarrows \text{Mg}^{23} + \gamma$ $\hspace{4cm}$ 7 579

$$[p\text{Na}^{22}]_\gamma = 3.0 \times 10^4 \, \rho_b \, T_9^{1/2} \exp\left(-8.99 \, T_9^{-1}\right)$$

$$\lambda_\gamma(\text{Mg}^{23}) = 3.27 \times 10^{10} \, [p\text{Na}^{22}]_\gamma \, \rho_b^{-1} \, T_9^{3/2} \exp\left(-87.95 \, T_9^{-1}\right)$$

(58) $\quad \text{He}^4 + \text{Na}^{22} \rightleftarrows p + \text{Mg}^{25}$ $\hspace{4cm}$ 3 144

$$[\text{He}^4\text{Na}^{22}] = [\text{He}^4\text{Na}^{20}]$$

$$[p\text{Mg}^{25}] = 3.85 \, [\text{He}^4\text{Na}^{22}] \exp\left(-36.49 \, T_9^{-1}\right)$$

(59) $\quad \text{He}^4 + \text{Mg}^{22} \rightleftarrows p + \text{Al}^{25}$ $\hspace{4cm}$ 3 927

$$[\text{He}^4\text{Mg}^{22}] = 5.0 \times 10^{20} \, \rho_b \, T_9^{-2/3} \exp\left(-53.1 \, T_9^{1/3}\right)$$

$$[p\text{Al}^{25}] = 0.550 \, [\text{He}^4\text{Mg}^{22}] \exp\left(-45.57 \, T_9^{-1}\right)$$

(60) $\quad p + \text{Na}^{23} \rightleftarrows \text{He}^4 + \text{Ne}^{20}$ $\hspace{4cm}$ 2 379

$$[p\text{Na}^{23}] = 6.0 \times 10^5 \, \rho_b \, T_9^{1/2} \exp\left(-3.93 \, T_9^{-1}\right)$$

$$[\text{He}^4\text{Ne}^{20}]_p = 1.24 \, [p\text{Na}^{23}] \exp\left(-27.61 \, T_9^{-1}\right)$$

16

TABLE 2—*Continued*

$Q(\text{MeV})$

(61) $\quad p + \text{Mg}^{23} \rightleftarrows \text{Al}^{24} + \gamma$
<div align="right">1 717</div>

$$[p\text{Mg}^{23}]_\gamma = 1.9 \times 10^3 \, \rho_b \, T_9^{1/2} \exp(-9.75 \, T_9^{-1})$$

$$\lambda_\gamma(\text{Al}^{24}) = 2.50 \times 10^{10} \, [p\text{Mg}^{23}]_\gamma \, \rho_b^{-1} \, T_9^{3/2} \exp(-19.93 \, T_9^{-1})$$

(62) $\quad \text{He}^4 + \text{Mg}^{23} \rightleftarrows p + \text{Al}^{26}$
<div align="right">1 874</div>

$$[\text{He}^4\text{Mg}^{23}] = [\text{He}^4\text{Mg}^{22}]$$

$$[p\text{Al}^{26}] = 1.21 \, [\text{He}^4\text{Mg}^{23}] \exp(-21.75 \, T_9^{-1})$$

(63) $\quad p + \text{N}^{15} \rightleftarrows \text{O}^{16} + \gamma$
<div align="right">12 13</div>

$$[p\text{N}^{15}]_\gamma = 4.22 \times 10^8 \, \rho_b \, T_9^{-2/3} \exp(-15.2 \, T_9^{-1/3}) \, (1 + 0.0274 \, T_9^{1/3}$$
$$+ \, 2.98 \, T_9^{2/3} + 0.57 \, T_9) + 1.16 \times 10^4 \, \rho_b \, T_9^{-3/2} \exp(-3.68 \, T_9^{-1})$$

$$\lambda_\gamma(\text{O}^{16})_p = 3.64 \times 10^{10} \, [p\text{N}^{15}]_\gamma \, \rho_b^{-1} \, T_9^{3/2} \exp(-140.5 \, T_9^{-1})$$

In several reactions three nuclei are produced and the reverse of these reactions is usually included.

The total rate of change of abundance of nucleus i is therefore given by

$$\frac{1}{A_i}\frac{dX_i}{dt} = \pm \sum_j \frac{X_j}{A_j} \lambda_k(j) \pm \sum_{j \geq k} \frac{X_j}{A_j}\frac{X_k}{A_k}[jk] \pm \sum_{j \geq k \geq \ell} \frac{X_j}{A_j}\frac{X_k}{A_k}\frac{X_\ell}{A_\ell}[jk\ell], \quad (16)$$

with appropriate modifications for identical particles as noted above. Note that by using mass fractions rather than number densities, an extra term due to changes in volume is not needed in the rate equation. The technical problem in constructing equation (16) for each nuclear constituent is to obtain expressions for $\lambda_k(j), [jk]$, and $[jk\ell]$. A discussion of this process may be found in Appendix B and more details will be found in Fowler, Caughlan, and Zimmerman (1967).

It is of interest to compare the reaction rates we have employed with those used by Fermi and Turkevich in 1950. In the intervening period a considerable amount of experimental evidence has been obtained for reaction rates on which they were compelled to make theoretical or semi-empirical estimates and new reaction mechanisms have been discovered. For the most important reactions involved, the approximate ratios between our rates and those of Fermi and Turkevich can be expressed as follows: for all four reactions in D(n,γ)T(p,γ)He^4 and D(p,γ)He^3(n,γ)He^4, a factor of $\sim$10; for D(D,γ)He^4, a factor of $\sim 10^{-3}$, for He^3(He^3,2p)He^4, a factor of 10^{-2}, and for He^3(He^4,γ)Be^7, a factor of $\sim$100. It will be clear that the last two factors mentioned aid considerably in bridging the mass gap at $A = 5$. Furthermore Fermi and Turkevich did not consider Be^7(He^4,γ)C^{11}, which we have found is effective in bridging the mass gap at $A = 8$ since Be^7(p,γ)B^8 remains in equilibrium with B^8(γ,p)Be^7 because of the low value of $Q = 0.135$ MeV. In addition they did not consider 3 He$^4 \rightarrow$ C$^{12} + \gamma$, which is well known to be effective in bridging both mass gaps at relatively high densities.

In constructing $\lambda_k(j), [jk]$, and $[jk\ell]$, the appropriate distribution functions for particles and photons at the same temperature T are used, since they are in thermal equilibrium.

The rate equations provide us with n first-order differential equations giving the time rate of change of each of the n mass fractions. In principle, these will provide a unique solution by numerical integration from chosen initial conditions. However, if the loss (or gain) rate per nucleus becomes much larger than the expansion rate, the loss rate

EXOERGIC DIRECTION ⟶
WEAK REACTION - - - ⟶

FIG. 2a.—Flow diagram indicating reactions included. Most inverse reactions have also been included except in the case of the nuclear beta-decays. For all nuclei heavier than B^{10}, the other initial nucleus is either a proton or He^4.

FIG. 2b.—Details of the reactions among the very light nuclei which are included in the calculation. All inverse reactions have also been included.

quickly balances the gain rate, and the equilibrium mass fraction appropriate to the instantaneous temperature results. Since the computer must take finite time steps, it cannot accurately compute the small time derivative given by the difference between the large and varying, but almost equal, gain and loss rates. Therefore, if a given nucleus is in this equilibrium condition, its mass fraction is computed by solving the algebraic equation resulting from setting $(dX_i/dt)_T = 0$ in equation (16).

A further difficulty arises if one reaction strongly couples two or more constituents. In this case the particular reaction rate will dominate in the rate equation for the constituents involved, so that if the nuclei are in equilibrium through this reaction, only one independent relation exists between them. One or more sums of the rate equations involved must then be used to solve for the sum of the mass fractions involved. The original rate equation is used to find the smaller of the mass fractions, and then the sum is used to give the larger. The reactions which necessitate this procedure are those with large cross-sections and small energy releases.

The time steps were adjusted so that no constituent whose abundance was greater than 10^{-15} could vary by more than ~ 10 per cent during any one time step. The estimated accuracy thus achieved in the numerical integration of the rate equations was ~ 1 per cent for the protons and alpha-particles, and ~ 10 per cent for the remaining nuclei with $A \leq 17$. For the heavier nuclei, the accuracy is less due to the necessity of terminating the reactions at Al.

IV. INITIAL CONDITIONS

We are concerned with specifying initial conditions for two distinct problems: (1) a universe which emerges from a state of very high temperature; (2) a massive object, initially at low temperature, which collapses inward to a state of significantly higher temperature $(T_9)_{\max}$ and "bounces" back to a final state of lower temperature.

The initial temperature for the universal case is taken as $T_9 = 60$ $(Z = 0.1)$. This is high enough so that all nuclei are in statistical equilibrium with each other, making the composition independent of the previous history of the universe. The proton-neutron ratio is given by equation (3), obtained by setting $(dX_n/dt)_T = 0$ or $(dX_p/dt)_T = 0$ in their rate equations. Similarly, by considering the reactions $j + k = i + \gamma$ which control the abundance of nucleus i at this high a temperature, one obtains, neglecting factors of order unity in (A36),

$$X(i) \approx 10^{-10} X(j) X(k) \rho_b T_9^{-3/2} e^{Q/kT} , \qquad (17)$$

so that the initial abundances decrease rapidly with increasing mass number. Since we know the variations of T and T_ν with time from Table 1, it is necessary to specify only the entropy of the photons per gram of baryons. This choice gives the parameter h. Calculations are then performed for various values of h. Recall that h relates ρ_b and T_9 in the later stages of the expansion, in accordance with equation (1). Integrations are carried down to a temperature $(T_9 \approx 0.01)$ where the abundances have become constant.

In the case of a massive star, we set $\rho_\nu = 0$ throughout the calculation. Integration begins at a low enough temperature $(T_9 \approx 0.01)$ to prevent reactions from immediately affecting the specified initial abundances. Again we must specify the parameter h (see § VII). The third quantity which must be specified is the temperature at which the system "bounces." The collapse rate is given by equation (4) until this temperature is reached, at which point the velocity is reversed, and the expansion rate again given by equation (4). Again integration proceeds to the final temperature $T_9 \approx 0.01$. In several cases alternative collapse and expansion rates have been used as discussed in § IX.

V. RESULTS FOR THE UNIVERSAL FIREBALL

In this section we shall discuss our results in the case of a universe containing non-degenerate neutrinos. The evolution of the abundances of the various nuclei during a typical run is illustrated in Figure 3, which covers only the time interval during which the mass fractions were changing appreciably. The final abundances by mass (if $>10^{-12}$) for various values of h are given in Tables 3A and 3B and plotted in Figure 4. The symbols ρ_0, q_0, and T_0 indicate the present density, deceleration parameter, and temperature, respectively. We have also used $\theta = T_0/3° \text{K}$ to express T_0 in terms of the currently fashionable value for the universal temperature. The long-lived β-decays of T, Be^7, and Na^{22} are taken into account at the end of the integration by adding their abundances to those of the daughter nuclei, He^3, Li^7, and Ne^{22}.
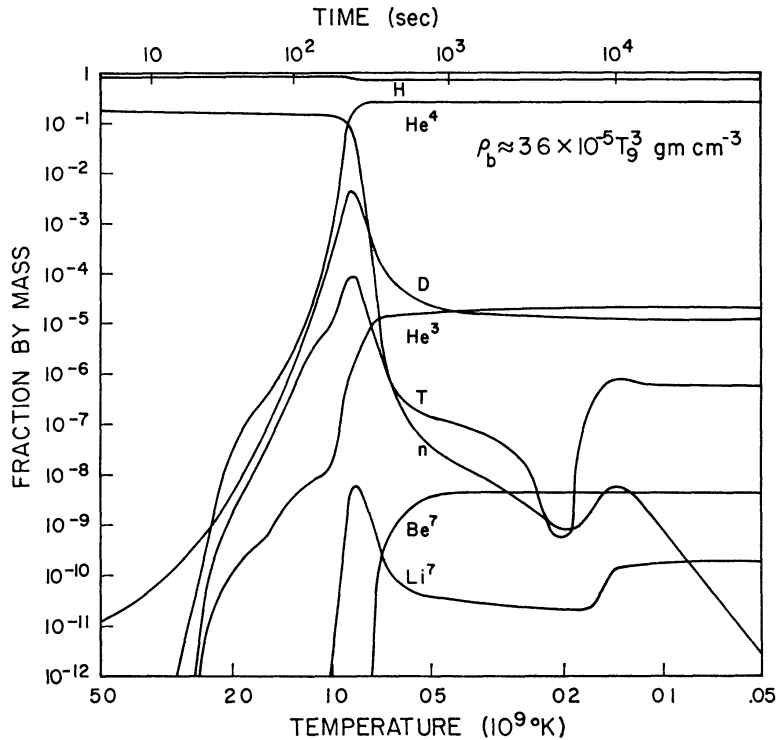
FIG. 3.—Evolution of abundances during the expansion of a typical low-density universe ($h = 3.6 \times 10^{-5}$, $q_0 = 0\ 026$ for $T_0 = 3°$ K).

TABLE 3A

ELEMENT PRODUCTION IN "LOW-DENSITY" UNIVERSES

$h.$	$3\ 64\times10^{-8}$	$1\ 15\times10^{-7}$	$3\ 64\times10^{-7}$	$1\ 15\times10^{-6}$	$3\ 64\times10^{-6}$	$1\ 15\times10^{-5}$	$3\ 64\times10^{-5}$	$1\ 15\times10^{-4}$	$3\ 64\times10^{-4}$
ρ_0/θ^3	$1\ 0\ \times10^{-33}$	$3\ 1\ \times10^{-33}$	$1\ 0\ \times10^{-32}$	$3\ 1\ \times10^{-32}$	$1\ 0\ \times10^{-31}$	$3\ 1\ \times10^{-31}$	$1\ 0\ \times10^{-30}$	$3\ 1\ \times10^{-30}$	$1\ 0\ \times10^{-29}$
q_0/θ^3	$2\ 6\ \times10^{-5}$	$8.2\ \times10^{-5}$	$2\ 6\ \times10^{-4}$	$8\ 2\ \times10^{-4}$	$2\ 6\ \times10^{-3}$	$8\ 2\ \times10^{-3}$	$2\ 6\ \times10^{-2}$	$8\ 2\ \times10^{-2}$	$2\ 6\ \times10^{-1}$
H..	$0\ 980$	$0\ 952$	$0\ 892$	$0\ 807$	$0\ 763$	$0\ 748$	$0\ 737$	$0\ 728$	$0\ 719$
D	$1\ 5\times10^{-2}$	$1\ 5\times10^{-2}$	$9\ 1\times10^{-3}$	$3\ 2\times10^{-3}$	$6\ 2\times10^{-4}$	$8\ 9\times10^{-5}$	$1\ 2\times10^{-5}$	$2\ 7\times10^{-7}$	$2\ 5\times10^{-12}$
He^3	$1\ 8\times10^{-4}$	$3\ 8\times10^{-4}$	$3\ 6\times10^{-4}$	$1\ 8\times10^{-4}$	$6\ 3\times10^{-5}$	$3\ 8\times10^{-5}$	$2\ 1\times10^{-5}$	$9\ 9\times10^{-6}$	$5\ 6\times10^{-6}$
He^4	$4\ 2\times10^{-3}$	$3\ 2\times10^{-2}$	$9\ 8\times10^{-2}$	$0\ 190$	$0\ 236$	$0\ 252$	$0\ 263$	$0\ 272$	$0\ 281$
Li^7	$9\ 7\times10^{-12}$	$5\ 1\times10^{-10}$	$3\ 3\times10^{-9}$	$3\ 4\times10^{-9}$	$5\ 2\times10^{-10}$	$2\ 1\times10^{-10}$	$4\ 4\times10^{-9}$	$2\ 1\times10^{-8}$	$4\ 3\times10^{-8}$

TABLE 3B

Element Production in "High-Density" Universes or Massive Stars Emerging from Very High Temperatures*

h	$1\ 15\times10^{-3}$	$3\ 64\times10^{-3}$	$1\ 15\times10^{-2}$	$3\ 64\times10^{-2}$	$1\ 15\times10^{-1}$	$3\ 64\times10^{-1}$	$1\ 15$	$3\ 64$	$11\ 5$
ρ_0/θ^3	$3\ 1\times10^{-29}$	$1\ 0\times10^{-28}$	$3\ 1\times10^{-28}$	$1\ 0\times10^{-27}$	$3\ 1\times10^{-27}$	$1\ 0\times10^{-26}$	$3\ 1\times10^{-26}$	$1\ 0\times10^{-25}$	$3\ 1\times10^{-25}$
q_0/θ^3	$0\ 82$	$2\ 6$	$8\ 2$	26	82	$2\ 6\times10^{2}$	$8\ 2\times10^{2}$	$2\ 6\times10^{3}$	$8\ 2\times10^{3}$
H	$0\ 709$	$0\ 701$	$0\ 691$	$0\ 681$	$0\ 670$	$0\ 660$	$0\ 648$	$0\ 631$	$0\ 603$
D									
He³	$4\ 4\times10^{-6}$	$3\ 5\times10^{-6}$	$2\ 4\times10^{-6}$	$1\ 0\times10^{-6}$	$1\ 7\times10^{-7}$	$5\ 7\times10^{-9}$	$2\ 7\times10^{-12}$		
He⁴	$0\ 291$	$0\ 299$	$0\ 309$	$0\ 319$	$0\ 330$	$0\ 340$	$0\ 352$	$0\ 369$	$0\ 397$
Li⁷	$1\ 1\times10^{-7}$	$2\ 9\times10^{-7}$	$6\ 8\times10^{-7}$	$1\ 1\times10^{-6}$	$8\ 1\times10^{-7}$	$3\ 4\times10^{-7}$	$5\ 9\times10^{-9}$	$1\ 4\times10^{-12}$	
B¹¹	$4\ 6\times10^{-12}$	$1\ 7\times10^{-11}$	$4\ 8\times10^{-11}$	$7\ 6\times10^{-11}$	$3\ 9\times10^{-11}$	$3\ 7\times10^{-12}$			
C¹²	$1\ 6\times10^{-12}$	$3\ 9\times10^{-11}$	$7\ 7\times10^{-10}$	$9\ 6\times10^{-9}$	$5\ 3\times10^{-8}$	$2\ 0\times10^{-7}$	$2\ 0\times10^{-7}$	$8\ 6\times10^{-8}$	$3\ 3\times10^{-8}$
C¹³		$3\ 6\times10^{-11}$	$8\ 4\times10^{-10}$	$1\ 1\times10^{-8}$	$7\ 3\times10^{-8}$	$2\ 5\times10^{-7}$	$2\ 2\times10^{-7}$	$9\ 6\times10^{-8}$	$4\ 3\times10^{-8}$
N¹⁴		$8\ 9\times10^{-12}$	$2\ 0\times10^{-10}$	$3\ 2\times10^{-9}$	$2\ 8\times10^{-8}$	$1\ 4\times10^{-7}$	$1\ 5\times10^{-7}$	$7\ 7\times10^{-8}$	$3\ 2\times10^{-8}$
N¹⁵					$1\ 1\times10^{-12}$	$3\ 7\times10^{-12}$	$3\ 7\times10^{-12}$	$1\ 9\times10^{-12}$	
O¹⁶			$9\ 2\times10^{-12}$	$2\ 4\times10^{-10}$	$2\ 6\times10^{-9}$	$2\ 2\times10^{-8}$	$9\ 1\times10^{-8}$	$1\ 3\times10^{-7}$	$4\ 6\times10^{-8}$
O¹⁷							$2\ 1\times10^{-12}$	$2\ 9\times10^{-12}$	$1\ 2\times10^{-12}$
Ne²¹					$2\ 9\times10^{-12}$	$2\ 6\times10^{-11}$	$1\ 6\times10^{-10}$	$7\ 7\times10^{-10}$	$7\ 1\times10^{-10}$
Ne²²					$5\ 5\times10^{-12}$	$5\ 5\times10^{-11}$	$3\ 7\times10^{-10}$	$1\ 8\times10^{-9}$	$1\ 5\times10^{-9}$
≥Mg					$1\ 1\times10^{-10}$	$2\ 8\times10^{-9}$	$5\ 1\times10^{-8}$	$1\ 0\times10^{-6}$	$8\ 6\times10^{-6}$

* Mass fractions less than 10^{-12} are not entered

$$q_0/\theta^3$$

UNIVERSE NUCLEOSYNTHESIS
$$\rho_b \approx h\,T_9{}^3 \text{ gm cm}^{-3}$$
$$T_0 = 3\theta \text{ °K}$$

FRACTION BY MASS

SOLAR SYSTEM ABUNDANCES

$$\rho_0/\theta^3 \text{ (gm cm}^{-3}\text{)}$$
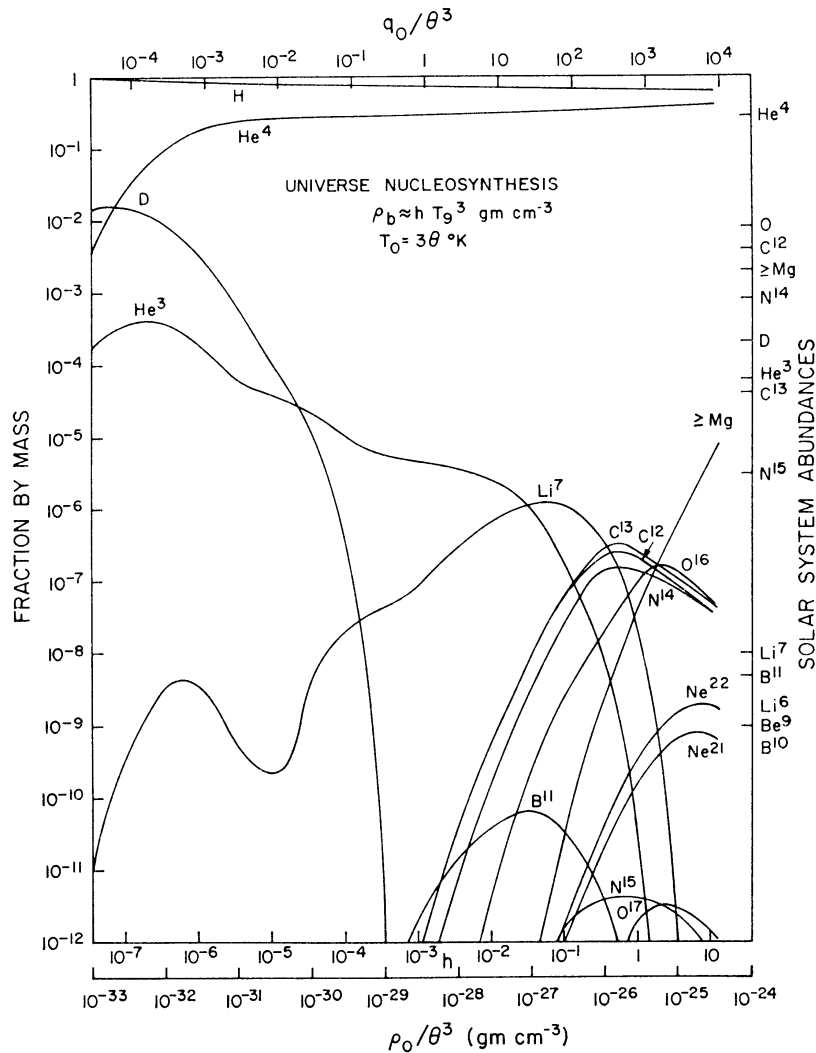
Fig. 4.—Element production in a universal fireball or a massive object expanding from $T_9 \geq 10$. The particular universe can be specified by either the parameter h, the present baryon density ρ_0 and photon temperature T_0, or the present deceleration parameter q_0 and T_0. The symbol θ represents $T_0/3°$ K, where the 3° K has been adopted from recent measurements at radio frequencies of a presumed universal background radiation. Solar-system abundances are given on the right-hand ordinate. For $h > 4$, Population II abundances are of order 10^{-2} of solar-system values.

For the present, we shall assume that the measurements of background radiation do indeed result from the expanded primeval fireball, so that $\theta = 1$. Then the observed upper limit (Sandage 1961) on the deceleration parameter, $q_0 \lesssim 3$, restricts us to "low density" universes, $h \lesssim 10^{-2}$. From Figure 4 we see that the only nuclei produced in significant quantities are D, He^3, He^4, and Li^7.

The route around mass 5, arising from the reactions $He^4(He^3,\gamma)Be^7$ and $He^4(T,\gamma)Li^7$, shows itself in the production of Li^7. The shape of the curve is due to the dominance of the former reaction at high densities and the latter at lower densities ($h < 10^{-5}$). Although an effective route around mass 8 does not appear to exist, it should be mentioned that the production of heavier elements in this range of h values depends most strongly on the reaction $Be^7(He^4,\gamma)C^{11}$, the cross-section for which has not been measured. The process $3\ He^4 \rightarrow C^{12}$ is ineffective at the densities under consideration. The values for D and He^4 are in good agreement with those obtained by Peebles (1966a, b). The values for He^3 and Li^7 are new.

TABLE 4

COMPARISON WITH OBSERVED ABUNDANCES

ELEMENT	WHERE OBSERVED	OBSERVED Mass FRACTION	CALCULATED MASS FRACTION FOR DIFFERENT q_0/θ^3		
			$5\ 0 \times 10^{-3}$	$1\ 0$	$2\ 6 \times 10^3$
D .	Earth	2×10^{-4}	2×10^{-4}	$< 10^{-12}$	$< 10^{-12}$
He^3	Meteorites	6×10^{-5}	5×10^{-5}	4×10^{-6}	$< 10^{-12}$
He^4	Sun*	$0\ 27$	$0\ 25$	$0\ 29$	$0\ 37$
Li^6	Earth (Li^6/Li^7)	1×10^{-9}	$< 10^{-12}$	$< 10^{-12}$	$< 10^{-12}$
Li^7	Meteorites	1×10^{-8}	3×10^{-10}	1×10^{-7}	1×10^{-12}
Be^9	Meteorites	1×10^{-9}	$< 10^{-12}$	$< 10^{-12}$	$< 10^{-12}$
B^{10} ..	Meteorites	1×10^{-9}	$< 10^{-12}$	$< 10^{-12}$	$< 10^{-12}$
B^{11}	Meteorites	5×10^{-9}	$< 10^{-12}$	4×10^{-12}	$< 10^{-12}$
C^{12}	Sun	4×10^{-3}	$< 10^{-12}$	$< 10^{-12}$	9×10^{-8}
C^{13}	Earth (C^{13}/C^{12})	4×10^{-5}	$< 10^{-12}$	$< 10^{-12}$	1×10^{-7}
N^{14}	Sun	8×10^{-4}	$< 10^{-12}$	2×10^{-12}	8×10^{-8}
N^{15} .	Earth (N^{15}/N^{14})	3×10^{-6}	$< 10^{-12}$	$< 10^{-12}$	2×10^{-12}
O	Sun	8×10^{-3}	$< 10^{-12}$	$< 10^{-12}$	1×10^{-7}
$\geq Mg$	Sun, meteorites	2×10^{-3}	$< 10^{-12}$	$< 10^{-12}$	1×10^{-6}

* From solar structure and evolution calculations.

A comparison of the results for three different universes with observed solar system abundances is made in Table 4. For the present, let us restrict our consideration to the elements whose abundance is calculated to be $\geq 10^{-12}$.

No single value of h reproduces the observed values, although the region $10^{-6} \lesssim h \approx q_0/(718\ \theta^3) \lesssim 10^{-4}$ yields a mixture in rough agreement with them. With $\theta \approx 1$, this range of h corresponds to $10^{-3} \lesssim q_0 \lesssim 10^{-1}$. The highest density case, $h = 10^{-4}$, with θ not much in excess of unity, is close to $q_0 = \frac{1}{2}$, the particular value that separates the open cosmologies from those that are closed. Evidently we must examine in some detail how far our calculations of the D, He^3, He^4, and Li^7 concentrations for this special case must be considered as discrepant from the values given in Table 3A. Placing the numbers in juxtaposition we have

	D	He^3	He^4	Li^7
Solar system . .	2×10^{-4}	6×10^{-5}	$0\ 27$	10^{-8}
Calculation ($h = 1\ 15 \times 10^{-4}$)	3×10^{-7}	1×10^{-5}	$0\ 27$	2×10^{-8}

To reconcile the cases of He³ and D it is necessary to argue that isotopic separation has taken place within the solar system. In the original planetary material the concentration of water vapor must have been ten times greater than the metallic content, in particular Mg, Si, Fe. Of the original water only about 1 part in 3×10^4 has been retained by the Earth. In whatever process led to the loss of water it is possible, as Urey (1952) has pointed out, the DHO was slightly less subject to fractionation than H_2O, and hence that D became concentrated in the small remaining fraction of the water. The value of D/H in terrestrial water would then be accidental and of no cosmological significance.

The value given in Table 4 for He³ was obtained by Signer and Suess (1964) from the analysis of a special class of gas-rich meteorites in which the concentrations of He, Ne, Ar, Kr, and Xe are too high to be attributable to a radiogenic origin or to spallation production by cosmic rays. Signer and Suess suggest that the grains of which the meteorites are composed may have been subject to bombardment by a primitive solar wind, the gas becoming trapped at the grain boundaries. On this picture the meteorites were built by a subsequent compacting of grains. The issue is evidently one of how far the He³/He⁴ ratio in the solar wind can be considered to be representative of the original primordial composition of the solar material. In particular, it is possible that evaporation into the solar wind is favored by the smaller mass of He³, in which case the He³/He⁴ ratio measured in these meteorites might be substantially higher than the primordial value.

Although the discrepancies in D and He³ might be explained along these lines, there are important counterarguments. The ratio D/H measured in meteorites appears to be close to the terrestrial value, which would be surprising if D/H has been subject to a large change through fractionation. Different samples might be expected to show different ratios. This issue is of such importance that more data on D/H in meteorites are needed. Especially is it important to insure that measured values have not been affected by contamination. The Ne/He ratios in the gas-rich meteorities are about $\frac{1}{300}$. Taking the solar helium abundance as 3×10^9 on the Si = 10^6 scale, this would indicate a Ne abundance of $\sim 10^7$, which is as high as the usually quoted value for the unfractionated solar neon abundance. Hence there does not seem to have been any appreciable fractionation between He and Ne, and therefore it is hard to maintain the existence of much fractionation between He³ and He⁴, unless the evaporation of the solar wind was controlled by an electromagnetic process, in which case the charge-to-mass ratio of ions may have played a significant role.

Unless we appeal to isotopic fractionation to overcome the discrepancies of D and He³ it is necessary to conclude that one or more of the following must hold good:

1. Our calculations contain appreciable inaccuracies.

2. The measured thermal radiation at 3° K is not primeval.

3. The parameter h is smaller than $\sim 10^{-4}$, q_0 is appreciably less than 0.5, and the cosmology is open.

4. The observed concentrations of D, He³, and Li⁷ are to be explained in terms of local processes, not in terms of cosmic synthesis.

5. At least one of our original assumptions is untrue.

The nuclear reaction rates for the very light nuclei involved in this section of our calculations are very well known. We are therefore reluctant to believe that the calculated values are subject to serious error.

There has so far been no general disposition on the part of physicists and astronomers to question the cosmological significance of the measurements of Penzias and Wilson, and of those of Wilkinson and Roll (see, however, Kaufman 1965 and Layzer 1966). We do not wish to do so here in any very serious respect, but we do think it worthwhile pointing out the following remarkable coincidence. The average spatial density of galactic material is $\sim 3-7 \times 10^{-31}$ gm cm⁻³ (Oort 1958). Of this, about one-third is probably helium, giving an average helium density of $\sim 10^{-31}$ gm cm⁻³. Since the conversion of 1 gm of hydrogen to helium yields $\sim 6 \times 10^{18}$ ergs, the average energy production—if the helium has

come from hydrogen—has been $\sim 6 \times 10^{-13}$ erg cm^{-3}. This energy density, *if thermalized*, would yield a temperature of just 3° K. Because in a cosmological expansion the baryon density decreases as R^{-3} while the radiation density decreases as R^{-4}, the coincidence is an accident if the measured 3° K is a relic of a cosmological fireball. On this view the expansion factor R has increased since the fireball by $\sim 10^9$ so that no such coincidence could have obtained over most of the expansion. It would be an accident of the present epoch. This is not the case if the observed radiation results from the thermalization of energy from recent hydrogen to helium conversion in stars. A thoroughgoing discussion relevant to this subject is given in Felten (1966).

Reducing h to 7×10^{-6}, in line with choice (3), we have the following comparison:

	D	He³	He⁴	Li⁷
Solar system	2×10^{-4}	6×10^{-5}	0 27	10^{-8}
Calculation	2×10^{-4}	5×10^{-5}	0 25	3×10^{-10}

The discrepancy in Li⁷ may not be too serious, because we can imagine inhomogeneities being present with higher values of h. Inhomogeneities operate in the sense that an effective contribution from higher values of h is much more likely than an effective contribution from lower values. This is because densities lower than the average make less contribution than densities which are higher than the average. The Li⁷ concentration can be brought into line if about 10 per cent of the material had an h value as high as 10^{-3}. Note also that h values both slightly lower and higher than this choice of 7×10^{-6} produce Li⁷ near the observed abundance.

For $\theta = 1$ and $h = 7 \times 10^{-6}$, $\rho_0 \approx 2 \times 10^{-31}$ gm cm^{-3}, very near the estimated 3-7×10^{-31} gm cm^{-3} for the average density of galactic material. Substitution in equation (9) gives $q_0 \approx 5 \times 10^{-3}$, and the cosmology is certainly open, by a considerable margin. The age of the galaxies on such a cosmological model would be close to $H_0^{-1} \approx 10$–13×10^9 years, for $H_0 = 75$–100 km (sec-Mpc)$^{-1}$. (We have used $H_0 = 100$ in computing q_0.) Considering the observational and theoretical uncertainties involved, this is in rough agreement with current estimates for the ages of the oldest stars in the Galaxy. It is also consistent with estimates from nuclear chronology by Fowler and Hoyle (1960). There are thus formidable reasons for supporting this cosmological model. These reasons are displayed together in Table 5.

TABLE 5

Open Cosmology with Background Temperature 3° K and
Deceleration Parameter $q_0 \approx 5 \times 10^{-3}$

$\rho_b \approx h T_9{}^3$ gm cm^{-3} $h \approx 7 \times 10^{-6}$

This value of h gives a production of D, He³, and He⁴ in good agreement with solar system abundances. Inhomogeneity can remove the discrepancy in Li⁷.

With $T = 3°$ K at the present epoch, $\rho_b \approx 2 \times 10^{-31}$ gm cm^{-3}, in good agreement with the average density of galactic material.

The age of the galaxies is $\sim H_0^{-1}$. With $H_0^{-1} \approx 10$–13×10^9 years, this age is consistent with estimates of the ages of the oldest stars in our own Galaxy, and with nuclear evidence for the age of the Galaxy.

How far can the issue be inverted? How far can Table 5 be construed as ruling out other systems of cosmology, for example, the cosmology $q_0 = +1$? The new item in Table 5 is the agreement of the calculated D, He³, He⁴ concentrations with solar-system values. The other items are, of course, well known. To deal with this question we must

now consider whether an alternative explanation of the D, He^3, and Li^7 concentrations is possible, as proposed in choice (4) above. The He^4 is relatively insensitive to h, so that agreement for He^4 is not a critical result, particularly as observational evidence exists for helium concentrations up to 0.4.

Beryllium is observed in stellar spectra. Beryllium is important because it is not produced in the universal fireball. Beryllium must be produced by spallation at stellar surfaces and He^3, Li^7 will also be generated along with the beryllium. The question is what concentrations of He^3 and Li^7 will be produced in this way?

The number of spallation events per second produced by high energy protons on a target nucleus i is proportional to

$$N_i \int \sigma_{ij}(E) \, n(E) \, v(E) \, dE \, ,$$

in which N_i is the density of target nuclei, σ_{ij} is the cross-section for production of a nucleus j, and $n(E) \, dE$ is the number of protons with energies between E and $E + dE$. The cross-section σ becomes small as E decreases below 100 MeV. On the other hand, it is reasonable to assume that $n(E)$ falls steeply as E increases above 100 MeV, so $E \approx 100$ MeV probably gives the main contribution to the integral.

We wish to compare the production of He^3 with Be^9. For He^3 the most effective target nucleus is He^4. For Be^9 the most effective targets are C^{12} and O^{16}. In stellar material He^4 is about 10^2 times as abundant as carbon and oxygen. Further, σ for the production of He^3 is more than 100 mb for protons of 100 MeV on He^4 whereas the cross-section for Be^9 production may well be as low as 1 mb. Combining these factors, we expect He^3 production to exceed that of Be^9 by a factor $\sim 10^4$.

A recent survey by Merchant (1966) of the Be abundances in the atmospheres of a number of stars gives values up to ~ 30 on the $Si = 10^6$ scale. The corresponding abundance of He^3 should therefore be $\sim 3 \times 10^5$, giving a mass concentration of $\sim 3 \times 10^{-5}$, not much different from the required value for the Sun.

There are two other possible explanations for the solar-system He^3 abundance. If the primitive D/H ratio in the Sun was 1.5×10^{-4} as found terrestrially, then the $D(p,\gamma)He^3$ reaction plus convective mixing has produced $He^3/He^4 = 1.5 \times 10^{-3}$ or $X(He^3)/X(He^4) \approx 10^{-3}$ in the solar surface. This is five times the mass fraction ratio given in Table 4. This result probably indicates that the primitive solar D/H ratio was not equal to the terrestrial value as discussed below in greater detail but the point must not be overlooked in the discussion of D and He^3 abundances. Finally, it is clearly possible for He^3 to have been produced in stellar nucleosynthesis, again by the $D(p,\gamma)He^3$ reaction, in this case taking place in regions in stars where $He^3(He^3,2p)He^4$ and $He^3(He^4,\gamma)Be^7$ are inoperative. The highly evolved models of Iben (1965a, b, 1966) and of Hayashi, Hōshi, and Sugimoto (1962) indicate that $X(He^3)/X(He^4) \sim 2 \times 10^{-3}$ in late stages of stars with masses in the range 1–5 $M_\odot$. This is ten times the solar system mass fraction ratio and might be taken to indicate that only 10 per cent of solar helium was produced in stars, but for our purposes the result at least indicates the possible copious production of He^3 in ordinary stellar nucleosynthesis.

On the basis of a spallation explanation for the abundance of the light nuclei, a positive result is also obtained for Li^7, which should be favored compared to Be^9 by a factor of at least 10. With ~ 30 for the Be abundance, a Li^7 abundance of ~ 300 can be expected. This exceeds the solar-system value by a factor of ~ 6.

Further evidence for spallation also comes from the presence of Li^6 in stars, for Li^6 is not synthesized in a fireball. According to Herbig (1964) the maximum observed ratio in stars for Li^6/Li^7 is $\sim \frac{1}{2}$, which corresponds to the spallation value. Herbig's results demonstrate the following result: In some, but not all, stars in which lithium is most abundant the ratio Li^6/Li^7 takes its spallation value. This shows that yields from spallation are comparable with the total Li concentration. Although at this stage we cannot eliminate the possibility that approximately equal contributions to lithium concentra-

tions come from spallation and from a universal fireball, the facts do weaken the case for lithium from a fireball.

It remains to discuss the case of D. The composition of solar material shows that some, if not all, of the solar material has passed through a previous generation of stars or of massive objects. This is necessary if we are to understand the detailed abundances that are present in the Sun. Moreover, the work of Salpeter (1959) and of Schmidt (1959) also indicates that much of the material of the Sun has passed through previous stars. Deuterium would not survive therefore in much of the material, even if D is adequately synthesized in a fireball, because D does not survive inside stars. Hence if D/H in the Earth is to be explained without isotopic fractionation in terms of the D/H value generated in a fireball the value of D/H at emergence from the fireball must be higher than the terrestrial value, say, $X(D)/X(H) \geq 3 \times 10^{-3}$. This would demand an uncomfortably low value of h, namely, $h \leq 10^{-6}$.

An alternative explanation of the origin of the terrestrial D in terms of spallation processes within the planetary material itself has been proposed by Fowler, Greenstein, and Hoyle (1962). At the present stage of the argument this alternative explanation still seems attractive.

We conclude that D, He^3, He^4, and Li^7 in solar-system abundances could well have been produced during the early stage of a universe with $h \approx 7 \times 10^{-6}$ and with $q_0 \approx 5 \times 10^{-3}$, $T_0 \approx 3° K$, and $\rho_b \approx 2 \times 10^{-31}$ gm cm^{-3} at the present time. However, there are a number of attractive alternative explanations for the solar-system abundances of the light nuclei. He^4 remains as the key nucleus in the possibility that nucleosynthesis took place during the early high-temperature stage of the universe. The He^4 content of Population II stars remains uncertain. In three stars located in the galactic halo Sargent and Searle (1966) find that the He/H ratio is lower by a factor of ~100 than it is in main-sequence stars of Population I. On the other hand, theoretical calculations on the structure and evolution of horizontal branch and RR Lyrae stars by Faulkner (1966) and Christy (1966) indicate that the He abundance needed to yield good agreement with observations is of the order of 20 to 30 per cent by mass.

VI. NEUTRINO DEGENERACY

Let us now consider the possibility that the universe is filled with enough neutrinos or antineutrinos to induce degeneracy (Zel'dovich 1964; Dicke *et al.* 1965). If either were completely degenerate up to some Fermi level Φ_ν, this would produce a mass density

$$\rho_\nu = \frac{\Phi_\nu^4}{8\pi^2 c^5 \hbar^3} = 2920 \, \Phi_\nu^4 (\text{MeV}) \text{ gm cm}^{-3} . \tag{18}$$

Thus we see that in order that the neutrino density be within the upper limit $\rho \lesssim 3 \times 10^{-29}$ gm cm^{-3} set by the observed deceleration of distant galaxies, the Fermi level at present can be at most $\sim10^{-2}$ eV. This is well within the upper limit of ~1 eV imposed by measurements of the very high-energy cosmic ray flux (Cowsik, Pal, and Tandon 1964).

The thermodynamic properties of partially degenerate neutrinos also depend on their temperature. However, partial degeneracy still allows them to interact sufficiently at temperatures $\gtrsim 10^{11} ° K$ so as to make their temperature equal to the photon temperature until the pairs annihilate. Therefore, in computing quantities involving the distribution function (A1) for neutrinos and antineutrinos, we have taken T_ν to be the same function of T as for the non-degenerate case. This is valid even in the completely degenerate case, since then the results are independent of T_ν.

As can be seen from the form of the distribution function (A1), the Fermi level Φ_ν and neutrino temperature T_ν both decrease as R^{-1} during the expansion. The quantity which shall be of interest to us is Φ_ν/kT, which thus remains constant, except during the pair annihilation.

Degeneracy affects element production in two ways. First, the increased density increases the expansion rate, allowing less time for the nuclear reactions to proceed. This is the only way in which the muon-neutrinos affect the problem. For simplicity we have only considered the case where $\Phi(\nu_\mu) = \Phi(\nu_e) = \Phi_\nu$, although values of $\Phi(\nu_\mu)$ greater than $\Phi(\nu_e)$ would change the results substantially through the effect on the time scale. Since $\rho_\nu \propto R^{-4}$ even under degeneracy, it is only necessary to compute the Fermi-Dirac integral at the starting temperature for a given choice of Φ_ν/kT.

Second, the reaction rates governing the interconversion of neutrons and protons ($\lambda_w(n)$ and $\lambda_w(p)$ in Table 2(a)) are altered. Electron-neutrino degeneracy results in a preponderance of protons, while electron-antineutrino degeneracy allows the neutrons to remain dominant until the Fermi level has decreased to the point where they can decay, ~ 1 MeV. Thus choosing a negative value of Φ_ν/kT determines the temperature at which element building can effectively begin. If the present photon temperature is $3°$ K, this would set $|\Phi_\nu/kT| \lesssim 40$, resulting in a "turn-on" temperature $\gtrsim 10^8$ ° K.

The element abundances were computed in the same manner as for the non-degenerate universes, after first choosing values for h and $(\Phi_\nu/kT)_0$, where the subscript denotes the (constant) value after the pairs annihilate. In the case of complete degeneracy, $|\Phi_\nu/kT_\nu| \gg 1$, the ratio of electron-lepton number to baryon number, denoted by $L_{e\nu}$, is related to these parameters by the simple expression

$$L_{e\nu} = P + 2.33 \times 10^3 \frac{(\Phi_\nu/kT)_0{}^3}{h}, \tag{19}$$

where P is the ratio of protons (including those within nuclei) to protons plus neutrons.

For "high-density" ($h > 10^{-3}$) universes with neutrino degeneracy ($\Phi_\nu > 0$), it is found that the abundances are even lower than those of Figure 4, due to the lack of neutrons. Therefore, we do not consider this case of much interest. High-density universes with antineutrino degeneracy ($\Phi_\nu < 0$), on the other hand, present the possibility of making substantial quantities of C, N, and O. This is due to the fact that element building can begin at a low enough temperature to prevent charged particle reactions from proceeding through the heavier nuclei. However, a buildup of heavier nuclei may still be possible through the fast β-decays of neutron-rich nuclei. A detailed analysis requires the inclusion of reactions other than we have considered here, and so remains for the future.

In Figures 5a and 5b are the results for two low-density universes, $h = 10^{-4}$ and 10^{-6}. The major effect of neutrino degeneracy ($\Phi_\nu > 0$) is a sharp drop in the He^4 abundance, followed by declines in the other abundances as the degeneracy is increased. Note that, for both values of h, the He^4 is reduced by a factor of 10 below the non-degenerate result for $(\Phi_\nu/kT)_0 = 1.4$.

In the case of antineutrino degeneracy, the He^4 reaches a maximum at $(\Phi_\nu/kT)_0 \approx -1.5$, corresponding to equal numbers of neutrons and protons being present at the time when the nuclear reactions can begin to produce He^4. As the degeneracy is increased, the protons are produced at lower temperatures, so that the charged particle reactions have increasing difficulty in building up the heavier nuclei. Finally, even the deuterium is reduced due to the lowering of the density at which it can be produced.

Thus we see that both small positive values and large negative values of $(\Phi_\nu/kT)_0$ can reduce the He^4 to that seen in the helium-poor stars (Sargent and Searle 1966; Greenstein 1966). However, the negative values appear to produce too much D and He^3 unless essentially no He^4 is allowed.

VII. MASSIVE STARS

The dynamical behavior of massive objects can be understood from Table 6, in which we consider how various quantities change under a homologous, adiabatic change of dimension. The ratio of specific heats γ for the gas is taken as $\frac{5}{3}$, while that for the
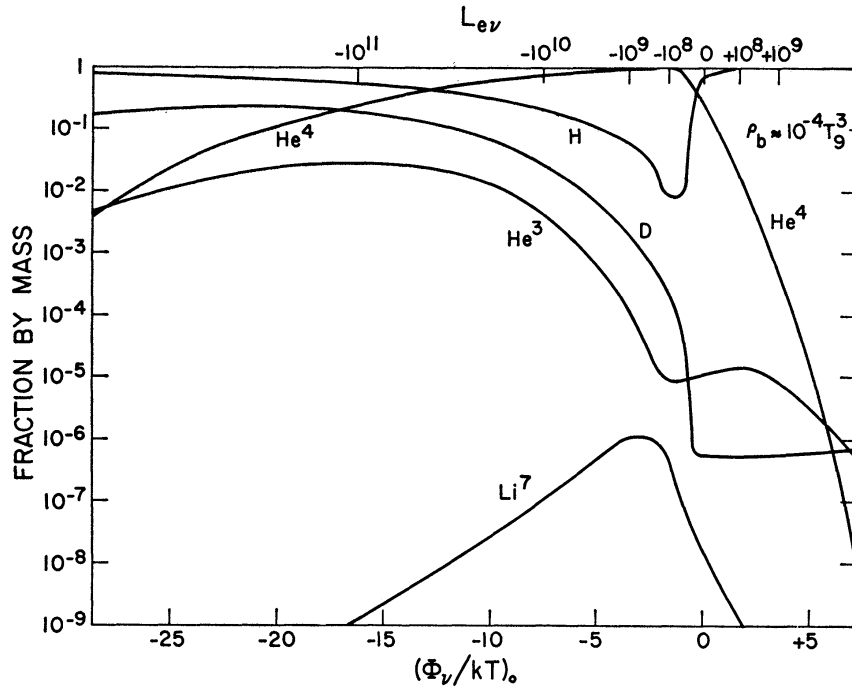
FIG. 5a.—Element production in a low density ($h = 10^{-4}$) universe in the case of neutrino ($\Phi_\nu > 0$) and antineutrino ($\Phi_\nu < 0$) degeneracy. The Fermi level of the electron neutrinos is denoted by Φ_ν, while T is the photon temperature, and the subscript refers to the value after the pairs annihilate. $L_{e\nu}$ is the ratio of electron lepton number to baryon number.
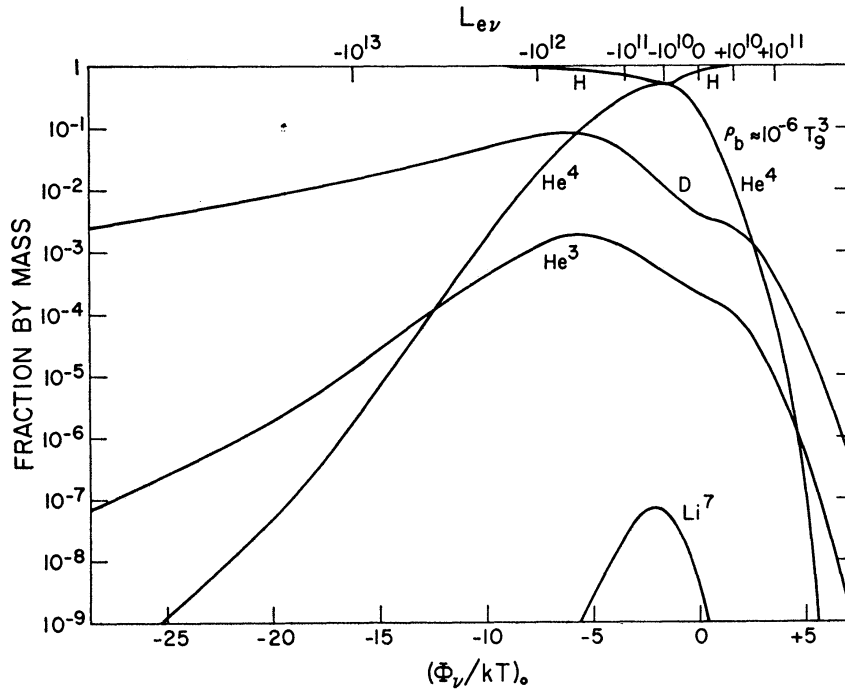

FIG. 5b.—Same as Fig. 5a except $h = 10^{-6}$

radiation field is $\frac{4}{3}$. Part I of Table 6 portrays the case when radiation makes a negligible contribution to the mass of the object, Part II the case when matter makes a negligible contribution. Radial changes in a spherically symmetric object are considered as well as one-dimensional changes in the smaller dimension of a flattened object.

Confining ourselves for the moment to the first part of the table, we note the curious circumstance that for spherically symmetric changes both the radiation pressure gradient (erg cm^{-4}) and gravitational force density (erg cm^{-4}) have the same dependence on the scale factor ξ. It follows that, when the main contribution to the pressure comes from radiation, these terms do not come into balance if they are initially out of balance. Equilibrium can be reached through the minor contribution of the gas pressure, provided

TABLE 6

BEHAVIOR OF VARIOUS FORCES WITHIN A MASSIVE STAR
UNDER ADIABATIC CHANGES OF DIMENSION

PART I: NEGLIGIBLE CONTRIBUTION OF RADIATION TO MASS OF OBJECT

Spherically Symmetric Change $\hspace{4cm} R \to \xi R$
    Gas pressure gradient $\propto \xi^{-(1+3\gamma)} = \xi^{-6}$
    Radiation pressure gradient $\propto \xi^{-5}$
    Gravitational force density $\propto \xi^{-5}$
    Centrifugal force density $\propto \xi^{-6}$

One-dimensional Change $\hspace{4cm} Z \to \xi Z$
    Gas pressure gradient $\propto \xi^{-(1+\gamma)} = \xi^{-8/3}$
    Radiation pressure gradient $\propto \xi^{-7/3}$
    Gravitational force density $\propto \xi^{-1}$

PART II: NEGLIGIBLE CONTRIBUTION OF MATTER TO MASS OF OBJECT

Spherically Symmetric Change $\hspace{4cm} R \to \xi R$
    Radiation pressure gradient $\propto \xi^{-5}$
    Gravitational force density $\propto \xi^{-7}$
    Centrifugal force density $\propto \xi^{-7}$

One-dimensional Change $\hspace{4cm} Z \to \xi Z$
    Radiation pressure gradient $\propto \xi^{-7/3}$
    Gravitational force density $\propto \xi^{-5/3}$

the two main terms are nearly equal. A disequilibrium involving a small difference may need a large value of ξ in order for the gas pressure term to make up the difference. Write

$$\beta = \frac{\text{Gas pressure}}{\text{Total pressure}} ; \qquad \Delta = \left| \frac{\text{Radiation pressure gradient}}{\text{Gravitational force density}} - 1 \right| .$$

The relative change of dimensions necessary to bring a disequilibrium into equilibrium is in general given by $\xi \approx \Delta/\beta$. Equilibria in which $\beta \ll 1$ may be described as "soft"— such equilibria are controlled by the minor gas pressure gradient term. In contrast, when $\beta \approx 1$ the total pressure gradient is effectively proportional to ξ^{-6}, and a small initial disequilibrium is corrected by a minor adjustment of ξ. Such equilibria are "hard."

If $\Delta \gg \beta$ the system may fail to find any equilibrium at all. Collapse inward or expansion outward to infinity occurs in such cases. Also when R is such that $2\,GM/Rc^2 > \beta$ a non-rotating system fails to find equilibrium (Chandrasekhar 1964; Fowler 1964, 1966; Wright 1964). The proportionality of the gravitational force density to ξ^{-5} includes only Newtonian gravitation. The post-Newtonian approximation, in which terms of the second order in the relativistic parameter $2\,GM/Rc^2$ are retained, adds a term that varies as

ξ^{-6}. Should this term exceed the term due to the gas pressure gradient, as it does when $2\,GM/Rc^2 \geq \beta$, the gas pressure term fails to stabilize the system.

These curious properties arise from the geometry of spherical symmetry. Table 6 shows the situation to be quite different in the one-dimensional case. Here a small disequilibrium is corrected by a small change of dimension, regardless of whether $\beta \approx 1$ or $\beta \ll 1$. The one-dimensional case is applicable to infalling massive objects with rotation. Provided rotary forces are not initially very small, the centrifugal force, being proportional to ξ^{-6}, eventually balances the component of the gravitational force toward the axis of rotation. Further collapse then follows the one-dimensional case. (By the rotation not being initially very small we mean that the centrifugal force must become important before R decreases so much that $2\,GM/Rc^2$ rises to unity, so that Newtonian arguments can be considered to hold good to an adequate approximation.)

An infalling massive object having sufficient rotation will "bounce," rather than fall into a state of equilibrium. This is because the dynamical energy of infall causes the equilibrium position to be overshot. The object falls in and bounces out again. The bounce is "hard" because the forces which oppose gravity are small during the infall and only become large at the bounce. The time scale is so short that energy losses are negligible. Furthermore, the energy released by nuclear reactions does not seriously raise the temperature for $h \lesssim 10^3$.

The matter density in our models is given by $\rho_b \approx hT_9{}^3$, while the radiation density $\rho_\gamma = 8.4\,T_9{}^4$. Therefore, for temperatures $T_9 \gtrsim 10^{-1}\,h$, most of the mass of the object is due to photons and possibly pairs, and we must refer to Part II of Table 6. Two interesting points emerge. First of all, we see that, if gravitational forces initially dominate over the radiation pressure, they will increase their relative strength during the ensuing collapse. In an actual body, whose mass is initially due to its matter density, the requirement that it be massive enough to initially collapse guarantees that the gravitational force will indeed dominate when it becomes a radiation sphere. It is easily seen that at this point the radius of the body has approached its Schwarzschild radius. The second point is the constancy of the ratio of gravitational and centrifugal forces. This would imply that rotation could not halt the radial collapse, if it were not for the fact that there will always be some contribution from the matter density. However, again this situation will be altered in the relativistic region.

In the one-dimensional case, we see as before that the pressure gradient will eventually halt collapse, although the bounce will not be quite as "hard" as in the matter density case. Thus we have the general result that a flattened configuration will always halt gravitational collapse, at least in the non-relativistic region.

We now wish to estimate the values that should be given to the parameter h in the bounce of a local object, and also consider the maximum temperature which can be attained at the bounce itself. Let us consider an initially spherical body which collapses to the radius R at which centrifugal force halts the collapse in two dimensions. Collapse then continues in the other dimension until bounce occurs for a flattened body of radius R, thickness $2Z$, and average density $\rho_m = (\rho_b + \rho_\gamma)_{\max}$. For a massive star, the major contribution to the pressure comes from the photons, so that $p \approx \frac{1}{3}\,aT^4$. Including the density and pressure of possible pairs will not significantly alter our results. We discuss six points which enable us to estimate or place limits on the quantities of interest.

1. The initial spherical collapse arises from the radiation of energy which continues at the onset of the general relativistic instability for $R \lesssim 2\,GM/\beta c^2$. In terms of the central temperature (Fowler 1964, 1966) the instability condition is

$$T_9 \gtrsim 2 \times 10^4 \left(\frac{M_\odot}{M}\right). \tag{20}$$

We are interested in central temperatures at which nuclear processes take place rapidly. In § VIII we discuss bounces at $T_9 \gtrsim 20$. The massive star must become unstable at

less than the bounce temperature. The conclusions reached thus apply for $M/M\odot \geq 10^3$. In § IX we discuss bounces at $T_9 \approx 0.5$ to 2 for which $M/M\odot \gtrsim 4 \times 10^4$ and $M/\widetilde{M}\odot \gtrsim 10^4$, respectively.

2. The initial spherical collapse becomes a spheroidal one under the influence of rotation and the general-relativistic instability is removed. Using the balance between pressure and gravitational forces which exists in the flattened body shortly before the bounce gives a rough estimate of the maximum density ρ_m and temperature T_m at bounce. We have

$$\frac{dp_m}{dZ} \approx 4\pi G \rho_m^2 Z .$$

Since the pressure is primarily due to radiation, to order of magnitude one can rewrite this equation as

$$\frac{dp_m}{dZ} \approx \frac{1}{3}\frac{aT_m^4}{Z} \approx 4\pi G \rho_m^2 Z \quad \text{or} \quad T_m^2 \approx \left(\frac{12\pi G}{a}\right)^{1/2} \rho_m Z .$$

But $M \approx 2\pi \rho_m R^2 Z$ so that

$$T_m \approx \left(\frac{3\, GM^2}{\pi a R^4}\right)^{1/4} . \tag{21}$$

3. Demanding that the body remain non-relativistic throughout the collapse so that a visible bounce can ultimately occur yields the inequality

$$\frac{2\,GM}{Rc^2} \lesssim 1 . \tag{22}$$

4. Combining equations (21) and (22) yields an upper limit on the bounce temperature as follows

$$T_m \lesssim \left(\frac{3\,c^8}{16\pi a G^3 M^2}\right)^{1/4}$$

or

$$T_{9m} \lesssim 10^4 \left(\frac{M\odot}{M}\right)^{1/2} . \tag{23}$$

5. An approximate but more detailed analysis of the binding energy required for hydrostatic equilibrium in a rotating body under general-relativistic conditions has been made. The exact results derived by Bardeen (1965) for a non-rotating object with polytropic index $n = 3$ and pressure/internal energy $= \Gamma_4 - 1 = \frac{1}{3}$ have been employed and the rotation has been treated in up to two orders beyond the Newtonian term using results of Bardeen and Anand (1966). It is found that the binding energy becomes very negative for small $\sigma = (p/\rho_b c^2)_c = (\Re T/\mu\beta)_c$ at the center but that the rotational terms can return the binding energy to zero for $\sigma \lesssim 0.4$ if differential rotation governed by the conservation of angular momentum for all mass elements (Fowler 1966) is permitted. If overshooting is neglected it can be assumed that the bounce occurs when the binding energy required for hydrostatic equilibrium returns to zero so that

$$T_{9m} \approx 5 \times 10^4 \sigma \left(\frac{M\odot}{M}\right)^{1/2} \lesssim 2 \times 10^4 \left(\frac{M\odot}{M}\right)^{1/2} , \tag{24}$$

which is very similar to the result in equation (23) above. From equations (20) and (24) one has

$$\left(\frac{M\odot}{M}\right) \lesssim \frac{T_{9m}}{2 \times 10^4} \lesssim \left(\frac{M\odot}{M}\right)^{1/2} . \tag{25}$$

6. Since the pressure is due to radiation the fundamental adiabatic relation $\rho_b \approx h T_9{}^3$ still holds, even during the one-dimensional collapse. If h is determined during hydrostatic equilibrium before collapse the results of Fowler and Hoyle (1964) show that

$$h \approx 10^5 \left(\frac{M_\odot}{M}\right)^{1/2},$$

(26)

or $h = 1, 10, 100, 1000$ for $M/M_\odot = 10^{10}, 10^8, 10^6, 10^4$ respectively. Combining equations (25) and (26) yields

$$2 \times 10^{-6} h^2 \lesssim T_{9m} \lesssim 0.2 h .$$

(27)

The upshot of the arguments of the present section can now be summarized. High-temperature bounces with $T_{9m} \approx 20$ are permitted for $100 \lesssim h \lesssim 3 \times 10^3$ or $10^3 \lesssim M/M_\odot \lesssim 10^6$. These are treated in the next section. In § IX we treat bounces in the range $0.5 \lesssim T_{9m} \lesssim 2$ during which significant nucleosynthesis occurs in the time scales permitted. The maximum in this range requires $10 \lesssim h \lesssim 10^3$ or $10^4 \lesssim M/M_\odot \lesssim 10^8$. The minimum in this range requires $2.5 \lesssim h \lesssim 500$ or $4 \times 10^4 \lesssim M/M_\odot \lesssim 1.6 \times 10^9$. Because of the order of magnitude nature of our analysis of the bounce we also give results for $h \approx 1$ or $M/M_\odot \approx 10^{10}$.

VIII. BOUNCES AT VERY HIGH TEMPERATURES

In this section we treat bounces in massive stars at very high temperatures which we have somewhat arbitrarily specified as $T_{9m} \gtrsim 20$. At the outset a comparison with the results of the universal fireball is instructive. We have seen from Figure 4 that a universal fireball with $h \lesssim 10^{-3}$ does not produce any nuclei with $A > 7$. The gap at mass 8 is not bridged. For larger h the gap can be bridged, however, because of the reactions $He^4 + Be^7 \to C^{11} + \gamma$ and $3 He^4 \to C^{12} + \gamma$, which become rapidly more important as h increases to values of order 10^2—i.e., for massive objects.

Let us estimate the relative importance of these two processes for making carbon, which then allows further synthesis to proceed. The reactions $He^3 + He^4 \rightleftarrows Be^7 + \gamma$ keep the Be^7 in equilibrium above $T_9 \approx 0.6$, which is also the temperature range where these processes are important. The Be^7 mass fraction is then given by

$$X(Be^7) = \frac{7 X(He^3) X(He^4) [He^3 He^4]}{12 \lambda_\gamma (Be^7)}$$

(28)

$$= 5.20 \times 10^{-11} X(He^3) X(He^4) \rho_b T_9{}^{-3/2} 10^{8 \, 00/T_9} .$$

The reaction $He^4 + Be^7 \to C^{11} + \gamma$ ($Q = 7.545$ MeV) then gives

$$\frac{dX(C^{11})}{dt} = \tfrac{11}{28} X(He^4) X(Be^7) [He^4 Be^7] .$$

This reaction should proceed mainly through the 8.10 MeV state in C^{11}, but the rate is unknown. Using formula (A32) in Appendix B, we have

$$[He^4 Be^7] \approx 9.5 \times 10^9 \rho_b T_9{}^{-3/2} [(2J+1) \Gamma_\gamma]_r 10^{-2 \, 80/T_9} .$$

(29)

Using equation (28), we then have

$$\frac{dX(C^{11})}{dt} = 0.195 [(2J+1) \Gamma_\gamma]_r X(He^4)^2 X(He^3) h^2 T_9{}^3 10^{5 \, 20/T_9} .$$

(30)

The reaction $3\,\mathrm{He}^4 \rightarrow \mathrm{C}^{12} + \gamma$ ($Q = 7.274$ MeV) gives

$$\frac{dX(\mathrm{C}^{12})}{dt} = \tfrac{1}{6} \times \tfrac{12}{64} X(\mathrm{He}^4)^3 [\mathrm{He}^4\mathrm{He}^4\mathrm{He}^4]$$

$$\approx 5.62 \times 10^{-10} X(\mathrm{He}^4)^3 h^2 T_9{}^3 10^{-1\,88/T_9}, \tag{31}$$

where we neglect the contribution of the second resonance in reaction rate (25) in Table 2(b). Therefore, the ratio of the rates is

$$\frac{dX(\mathrm{C}^{11})}{dt} \bigg/ \frac{dX(\mathrm{C}^{12})}{dt} \approx 3.5 \times 10^8 [(2J+1)\Gamma_\gamma]_r \left[\frac{X(\mathrm{He}^3)}{X(\mathrm{He}^4)}\right] 10^{7\,08/T_9}. \tag{32}$$

We have estimated $J = \tfrac{5}{2}$, $\Gamma_\gamma = 10^{-7}$ MeV,[4] giving

$$\frac{dX(\mathrm{C}^{11})}{dt} \bigg/ \frac{dX(\mathrm{C}^{12})}{dt} \approx 210 \left[\frac{X(\mathrm{He}^3)}{X(\mathrm{He}^4)}\right] 10^{7\,08/T_9}. \tag{33}$$

The relative strength is seen to be strongly temperature-dependent. Referring to the high-density part of Figure 4, it turns out that the metal ($\geq$ Mg) production is due to the triple-α reaction, while the lower-mass heavy elements are produced from the 10^{-7}–10^{-6} He^3 that is produced in the region $h \geq 10^{-1}$. The figure shows how the final abundance of He^3 drops as the production of these elements increases. In order for synthesis through this route to be effective, the C^{11} must form N^{12} through C^{11} (p,γ) or N^{14} through C^{11} (He$^4,p$) before it decays to B^{11}.

In the introductory section we remarked that Hayashi and Nishida (1956) found that C^{12} produced at high temperatures and densities is rapidly processed by reactions of the type C^{12}(p,γ)N^{13} (He$^4,p$)O^{16} (p,γ)F^{17} (He$^4,p$)Ne^{20}. . . . Our computations for objects emerging from temperatures $T_9 \geq 10$ confirm this result. We find that, when h becomes large enough for appreciable amounts of C^{12} to be produced by the triple-α reaction, the resulting carbon is rapidly processed into the metals. We attribute the weak metal concentrations found in the oldest stars to this process. Obviously such concentrations were not derived from previous stars of normal mass. Nor were they derived from a universal fireball if $T_0 = 3°$ K.

The only difference in the calculation of element production in a massive star bouncing at $T_{9m} \gtrsim 20$ and in the universe is the neglect of the neutrino density, which slightly increases the time scale and slightly changes the n-p weak reaction rate. Therefore, the results indicated on Figure 4 for $h > 1$ should apply in this case also. In particular, the metal production is seen to increase rapidly with h, in keeping with the dependence of the triple-α rate on $\rho_b{}^2$. In Figure 6 we present the abundance evolution for $h = 20$ within an object emerging from very high temperatures in which we did neglect the neutrino density. (Although this h value is slightly below the limits found in § VII, it illustrates the major points.) Recall that the initial conditions are set by statistical equilibrium.

We feel that these results contain a most significant point. The neutrons remain more abundant than the metals down to a temperature $T_9 = 4$. Since their mass fractions are equal at this point, there are of the order of 40 neutrons per metal nucleus present. This is sufficient to synthesize nuclei in significant abundances up to $A \approx 100$ but not higher. However, for the higher h values this occurs before the bulk of the metals is generated. As the temperature continues to fall, the neutrons drop out, and they have essentially disappeared at the stage where the metals are mainly synthesized. We find that, although the final metal abundance changes markedly as we vary h, the abundance of

[4] Recent measurements by Spanur (1966) on the 8.56 MeV "mirror" state in B^{11} indicate that $J = \tfrac{3}{2}$, $\Gamma_\gamma \approx 2 \times 10^{-6}$ MeV. The maximum production of C^{12}, C^{13}, N^{14}, O^{16}, $\geq$ Mg in Fig. 4 is thereby increased by approximately a factor of 2.

metals subject to an equal abundance of neutrons remains at $\sim 10^{-5}$ as we increase h above 20. The implications are: (1) a mass fraction of $\sim 10^{-5}$ of metals is subject to an r-process in which neutrons are added rapidly; (2) most of the metals remain in the iron group, because when they are synthesized too few neutrons remain to promote an r-process.

This process produces mass fractions of individual elements with $60 \lesssim A \lesssim 100$ of order 10^{-7}–10^{-6}. Thus we expect metal production in the iron group to be accompanied by a "tail" of heavier elements. Hence heavy elements should be present in material emerging from massive objects—provided the latter have bounced at high enough tem-
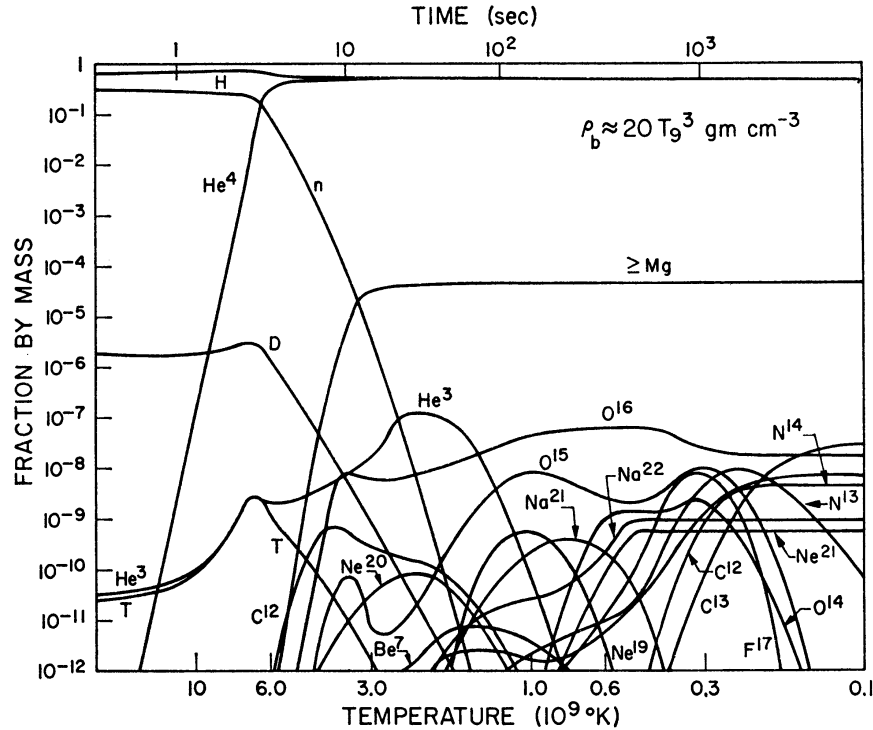
Fig. 6.—Evolution of abundances during the expansion from very high temperature of a typical massive object with $h = 20(M \approx 10^{8} M\odot)$.

peratures. Observational evidence that the heavy elements in old halo red giants do indeed cut off at $A \approx 100$ is discussed by Pagel (1965).

A determination of the precise composition of the metals and their "tail" goes beyond the immediate scope of the present paper. It is our intention to consider details in a future paper.

IX. BOUNCES AT $T_9 \approx 1$

Quite different results are expected in the case of a bounce occurring at a temperature where the abundances are not fixed. This is due to two factors: (1) The effect of the initial composition on the final abundances. It is assumed that the massive objects now under discussion formed from material enriched in elements heavier than hydrogen by nucleosynthesis in the universal fireball or in massive objects which bounced at very high temperature. (2) The strong Coulomb effects in the reaction rates.

In Figures 7–9 we give results for $h = 1, 10, 10^2, 10^3$ and $T_{9m} = 0.5, 0.7, 1.0$, and 2.0 for the following initial compositions:
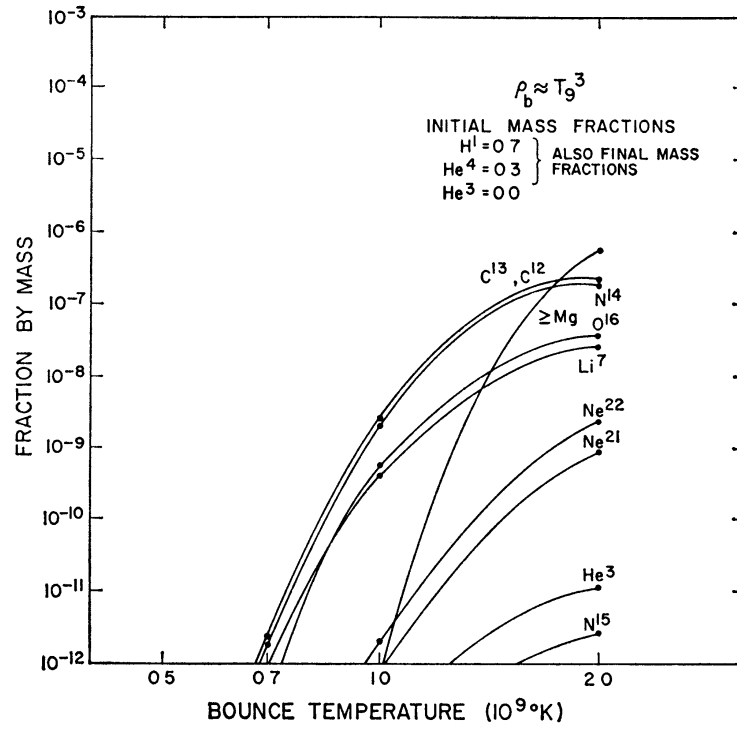
FIG. 7a.—Element production in massive local objects which bounce at temperatures in the range $0.5 \leq T_9 \leq 2\,0$ with initial composition $X(\mathrm{H}) = 0.7$, $X(\mathrm{He}^4) = 0.3$, and $X(\mathrm{He}^3) = 0$.
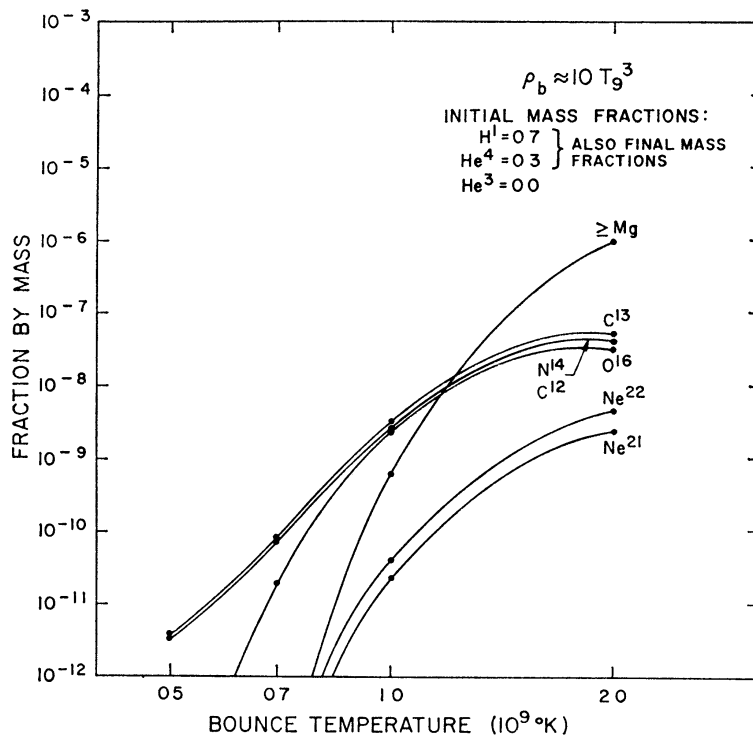
FIG. 7b.—Same as Fig. 7a

35
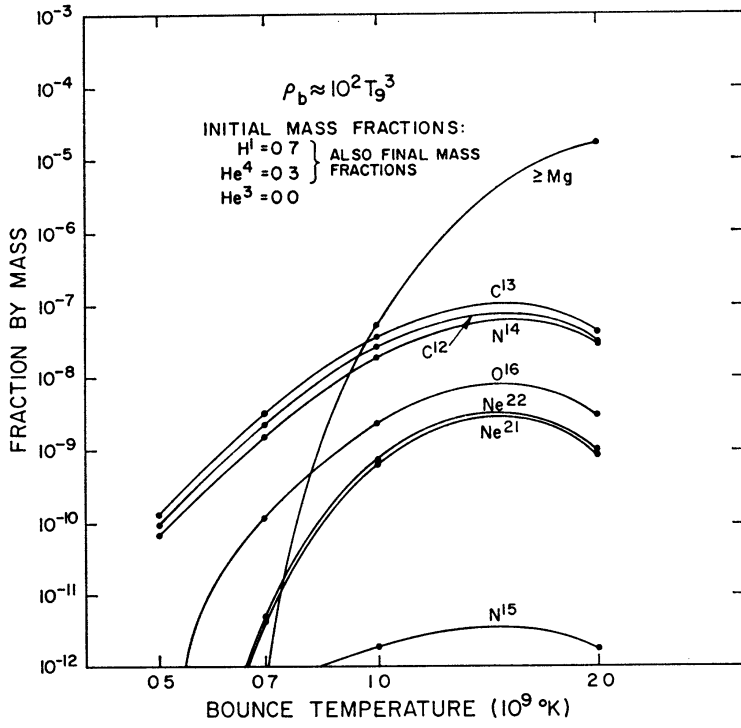
FIG. 7c.—Same as Fig. 7a
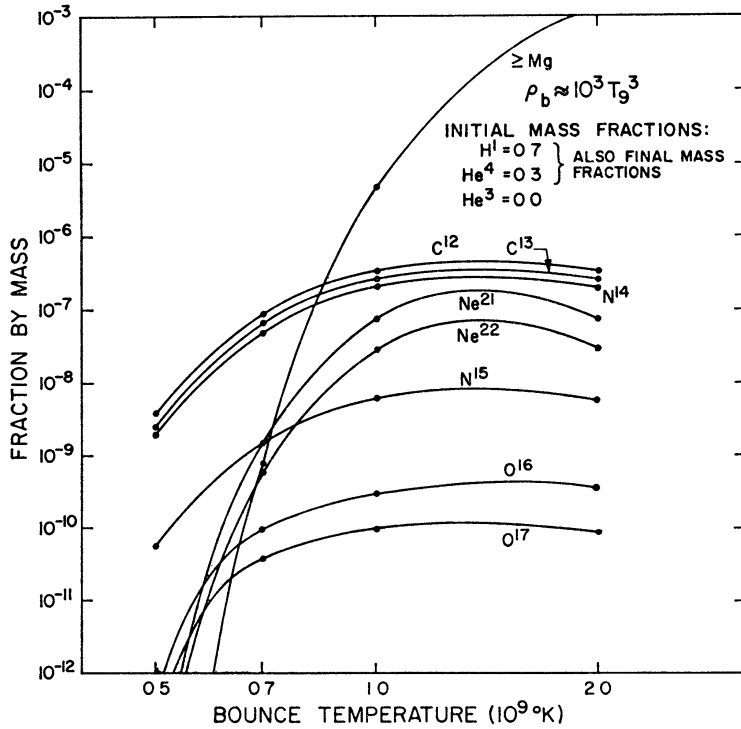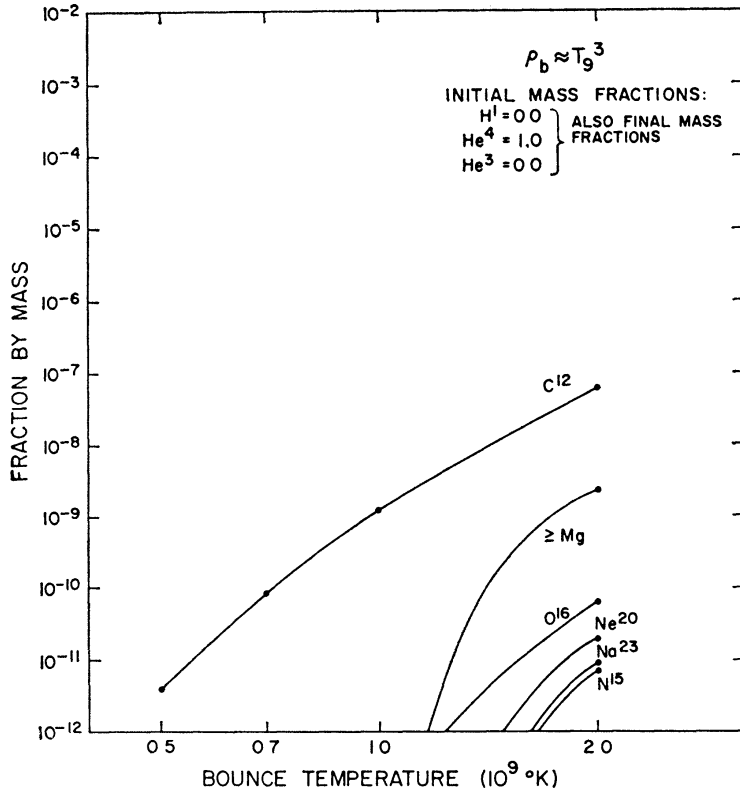

FIG. 7d.—Same as Fig. 7a

36

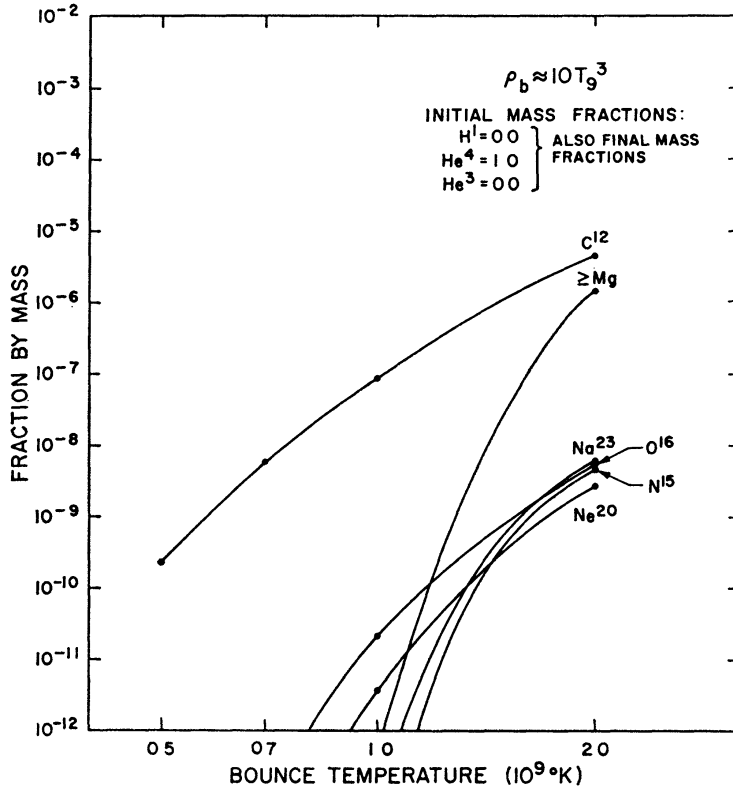FIG. 8a.—$X(H) = 0$, $X(He^4) = 1.0$, and $X(He^3) = 0$

FIG. 8b.—Same as Fig. 8a
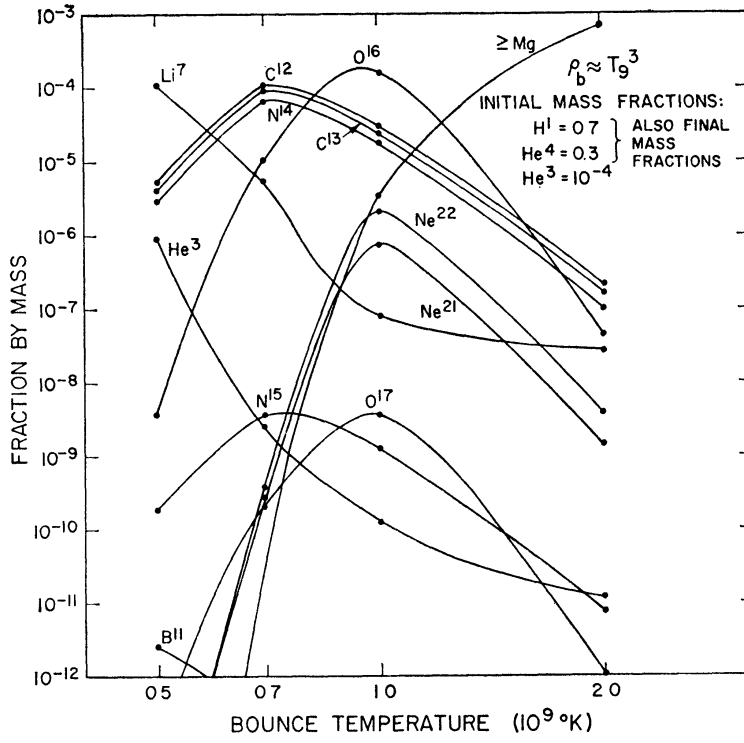
37
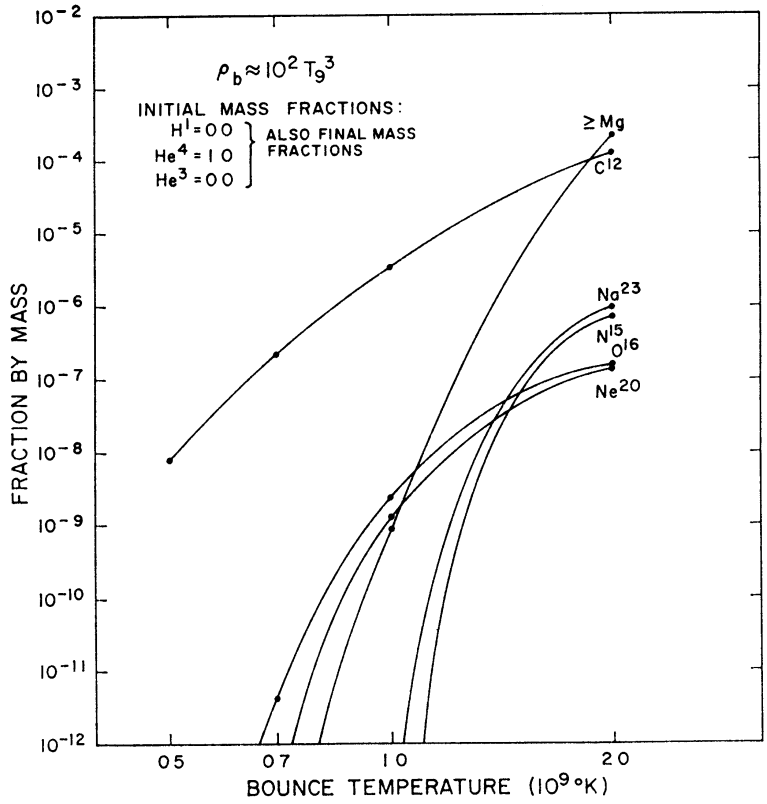
FIG. 8c.—Same as Fig 8a
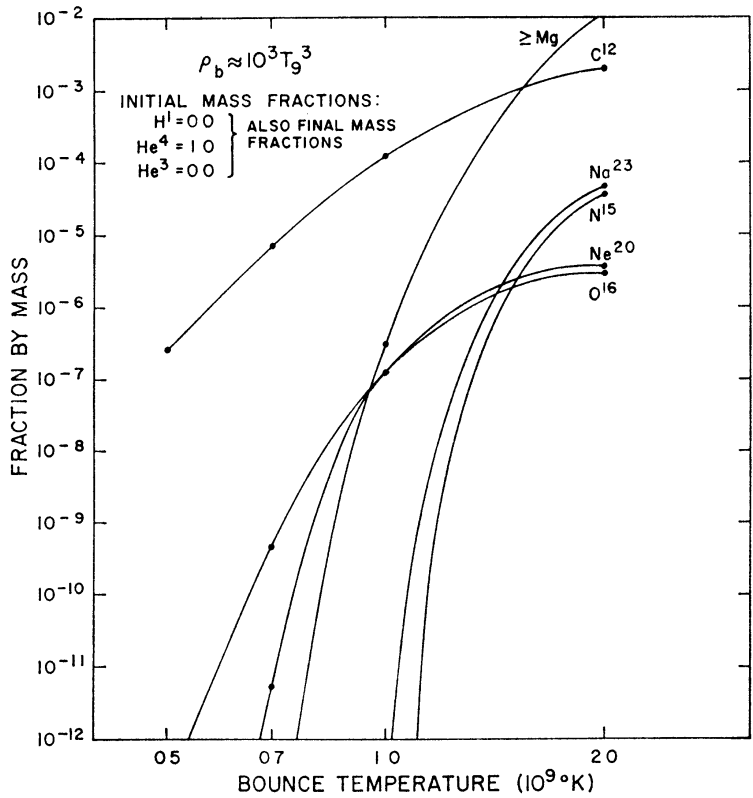
FIG. 8d.—Same as Fig. 8a

38

FIG. 9a.—$X(H) = 0.7$, $X(He^4) = 0 3$, and $X(He^3) = 10^{-4}$
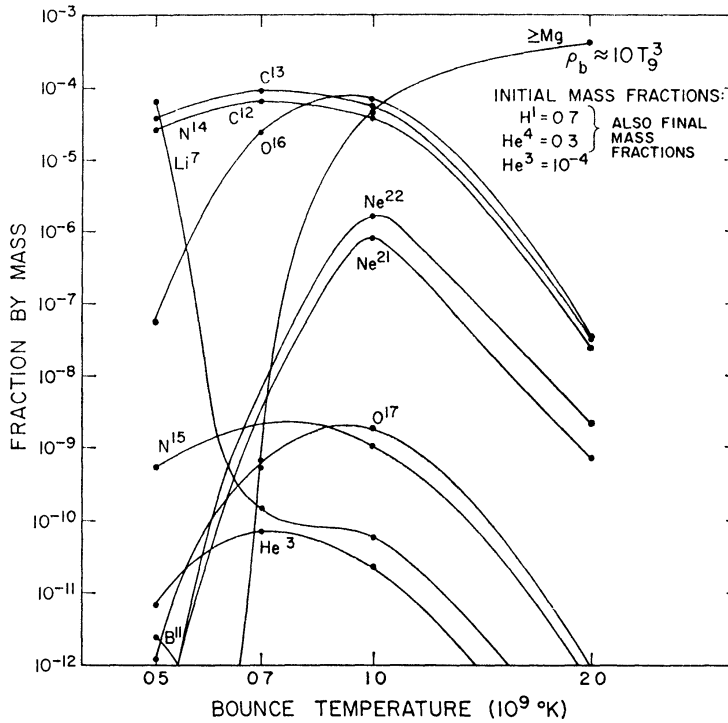
FIG 9b.—Same as Fig. 9a

39
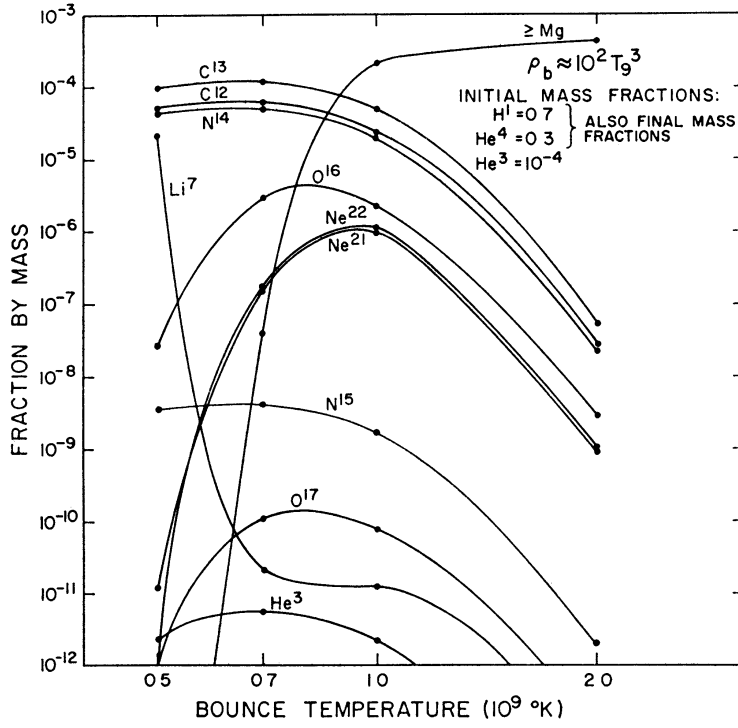
FIG. 9c.—Same as Fig. 9a
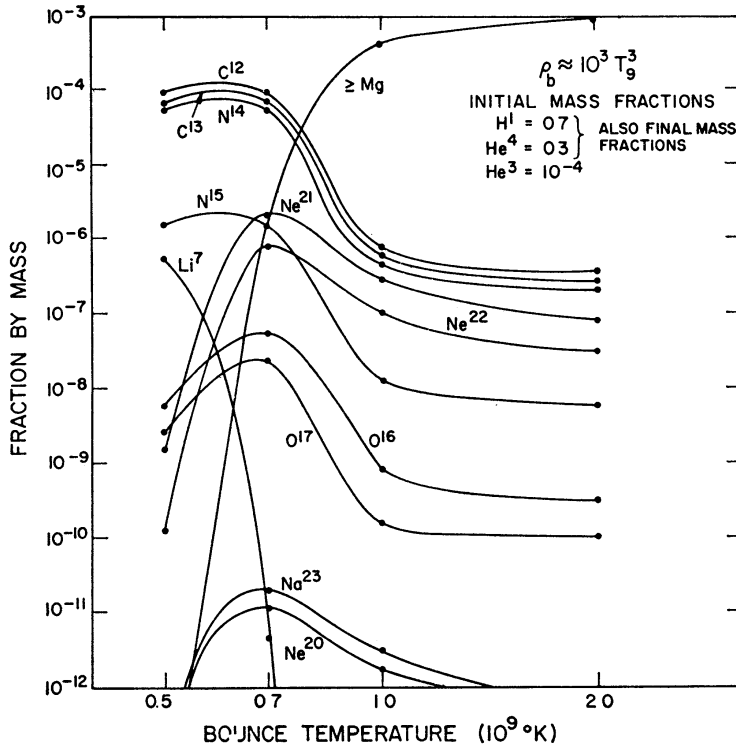
FIG. 9d.—Same as Fig. 9a

40

3W

1967ApJ...148....3W

Figures $7a$–$7d$: $X(p) = 0.7$, $X(\mathrm{He}^4) = 0.3$, all others $= 0$. Either the universal fireball or previous massive objects produced considerable He^4 but no He^3.

Figures $8a$–$8d$: $X(\mathrm{He}^4) = 1.0$, all others $= 0$. The He^4 core of a massive object which remained stable during hydrogen burning finally implodes due to relativistic effects.

Figures $9a$–$9d$: $X(p) = 0.7$, $X(\mathrm{He}^4) = 0.3$, $X(\mathrm{He}^3) = 10^{-4}$, all others $= 0$. The universal fireball produced considerable He^4 plus a small amount of He^3. (See what follows for further amplification.)

We have connected the computed values for the four temperatures by estimated curves. Let us now discuss these results in turn.

Figures $7a$–$7d$ and $8a$–$8d$ are curiously uninteresting. In Figures $7a$–$7d$, for $h \gtrsim 10^2$ and $T_{9m} \approx 2$ we obtain a significant amount of metals, which would be expected to be mostly in the region of Mg and Si at this temperature. Otherwise no element is produced in adequate quantities to explain even the low abundances observed in Population II stars. In Figures $8a$–$8d$, C^{12} is the only additional element produced in significant quantities at high h and T_{9m}, except perhaps for N^{15} and Na^{23} produced for $h = 10^3$ at $T_{9m} = 2$. The C^{12} survives because no protons are present.

Figures $9a$–$9d$ represent by far the most interesting case. The range $0.7 \lesssim T_{9m} \lesssim 1.0$ for $h \approx 10^2$, for example, gives average abundances of $\mathrm{C}^{13} \approx 10^{-4}$, $\mathrm{C}^{12} \approx 6 \times 10^{-5}$, $\mathrm{N}^{14} \approx 5 \times 10^{-5}$, $\mathrm{O}^{16} \approx 3 \times 10^{-6}$, Ne^{21}, $\mathrm{Ne}^{22} \approx 10^{-6}$, $\mathrm{Mg}^{24} \approx 3 \times 10^{-5}$, and perhaps $\mathrm{Si}^{28} \approx 10^{-5}$. Some relative abundances are seen to differ appreciably from these values for other choices of h and T_{9m}, however. At such temperatures we do not expect much synthesis beyond Si^{28}. The C, N, and $\geq$Mg abundances strikingly reflect the effect of the initial He^3 being converted into heavier elements. Below $T_9 \approx 1$, the low Q-value of O^{16} $(p,\gamma)\mathrm{F}^{17}$ and the Coulomb barrier for α-particles prevent synthesis from proceeding beyond oxygen. The O^{14} and O^{15} then decay to form carbon and nitrogen.

The higher temperature bounces discussed in the previous section, together with the results in Figures $9a$–$9d$, would give a reasonable approximation to all the elements observed in Population II stars. However, it is to be emphasized that Figures $9a$–$9d$ require He^3 or D to be present initially. (Any D present initially will be converted into He^3.) How could this have been the case? Two answers are possible: (1) The material of a massive bouncing object has already experienced very high temperatures in a universal fireball. (2) The He^4 in the material has been subject to extensive spallation. If possibility (2) could be eliminated, we should perhaps be able to arrive at the critical conclusion that conditions at low h, $h \lesssim 10^{-4}$, and $T_9 \geq 10$ have occurred, either in a universal fireball or possibly under unknown localized radiation conditions in which general relativity played a critical role. Elimination of the spallation possibility is difficult, as we have already shown in § V. It is particularly difficult to eliminate spallation under conditions where massive objects are collapsing in strong gravitational fields, since such conditions might be expected to lead to the extensive production of particles with relativistic energies. A strong radio source generates $\sim 10^{60}$ ergs in the form of such particles. If 1 per cent of this energy were used to produce He^3 from He^4, the quantity of He^3 would be of order 10^{40} gm, enough to give a concentration of $\sim 10^{-4}$ for He^3 throughout a galactic mass.

Some abundances in Figures $9a$–$9d$ are not at all like solar system abundances. Nitrogen is often as abundant as C^{12}, C^{12} is often more abundant than oxygen, $\mathrm{C}^{13} \approx \mathrm{C}^{12}$, and neon occurs as Ne^{21} and Ne^{22}. Could the first stars have possessed these curiosities? For stars of low surface temperature, the excess carbon would lead to carbon bands appearing in the spectrum. This is not seen in the cool giants of Population II, which would appear to be an objection to a direct association of the composition of Figures $9a$–$9d$ with the stars of globular clusters. On the other hand, C^{13} is not easily produced in ordinary stars. It is therefore of interest to find C^{13} appearing so prominently in the present calculations. It seems possible that the rare nuclei C^{13} and Ne^{21} were synthesized in massive objects under the conditions of Figures $9a$–$9d$. These nuclei are just the ones that experience

(He^4,n) reactions in stars, a circumstance that might well have promoted the early occurrence of an s-process in evolving stars (Pagel 1965).

In order to investigate the effects of expansion rates other than (4) on element production in massive stars, abundances were computed for an object with $h = 10^2$ which bounced at $T_9 = 1.0$. In one case, the rate (4) was multiplied by a factor proportional to $T_9^{3/2}$, appropriate to the flattening phase of a collapsing rotating body. In the other case, it was multiplied by a factor proportional to $T_9^{-1/2}$, appropriate to the early stages of collapse following the general-relativistic instability in a spherical body. In both cases, C, N, and Ne^{22} abundances were roughly proportional to the time scale near bounce. The O^{16} and Ne^{21} remained nearly constant, while the heavier elements ($\geq Mg$) varied roughly as the square of the time scale.

X. CONCLUSIONS

1. Helium is produced in a universal fireball as well as in massive objects which have bounced, provided that both emerged from temperatures $T_9 \gtrsim 20$. The mass fraction of He^4 produced lies between 0.2 and 0.3 for the universal fireball (assuming $T_0 \approx 3° K$), but can be higher in a massive object. It is therefore of great importance to determine helium concentrations in different astronomical bodies. A confirmation of $X(He^4) \approx 0.4$ for B stars and for some planetary nebulae could point toward massive objects as the site of origin for the helium. On the other hand, if it could be shown that $X(He^4)$ is always close to 0.27, this would be evidence favorable to a universal fireball.

2. D, He^3, and Li^7 are also produced in a universal fireball. The ratio He^3/He^4 appears to have been $\sim 2 \times 10^{-4}$ in the Sun at the time of formation of certain meteorites. This is explicable in terms either of spallation, synthesis in ordinary stars, or production in a fireball. In addition, if D/H was equal to the terrestrial value, 1.5×10^{-4}, in the primitive Sun, then He^3/He^4 should equal 1.5×10^{-3} now. The ambiguity regarding spallation and fireball production also applies to Li^7.

3. Elements heavier than Li^7 are not produced in significant quantities at low values ($\lesssim 10^{-2}$) of the parameter h, i.e., for $\rho_0/T_0^3 \lesssim 10^{-29}$.

4. Metals of the iron group are produced in massive objects which bounce at very high temperatures, $T_{9m} \gtrsim 20$. As the first of these metals are synthesized they are built by neutrons to still heavier elements ($60 \lesssim A \lesssim 100$) by a new kind of r-process. However, this process only affects a mass fraction of $\sim 10^{-5}$, for by the time the main bulk of the metals are synthesized the neutrons have disappeared.

5. Elements heavier than Mg^{24} are also synthesized at lower bounce temperatures, $T_{9m} \approx 2$, in massive objects initially composed of H and He^4. In this case, however, there are no neutrons to produce an r-process.

6. A massive object composed initially of essentially pure He^4 can also synthesize C^{12}, but little else that is of interest. This indicates the fact that $3 He^4 \rightarrow C^{12}$ can bridge the mass gaps at $A = 5$ and 8.

7. Significant quantities of Li^7, C^{12}, C^{13}, N^{14}, N^{15}, O^{16}, Ne^{21}, Ne^{22}, and metals are produced in massive objects having the range of parameters $1 \lesssim h \lesssim 10^3$ and $0.5 \lesssim T_{9m} \lesssim 2.0$, provided a concentration $\gtrsim 10^{-5}$ of He^3 is initially present in the material along with H and He^4. This is an example of the effectiveness of the reactions $He^3 (He^4,\gamma)Be^7 (He^4,\gamma)C^{11}$ in bridging masses 5 and 8 if sufficient He^3 is present, and the density and temperature are high enough.

8. None of the cases we have investigated in this paper produce abundances for $A \geq 12$ at all similar to the abundances found in the solar system and in Population I stars. This points strongly to these being due to stellar synthesis.

9. It is possible that the abundances obtained here are applicable to the oldest Population II stars, although there may be difficulty in explaining some of the relative abundances.

10. The abundances of D, He^3, He^4, and Li^7 calculated for $h \approx 7 \times 10^{-6}$ may be taken to support the view that a universal fireball existed in the early stages of the expansion of the universe. The evidence on this point is not unequivocal, however. If the present radiation temperature $\approx 3°$ K, this value of h corresponds to a present deceleration parameter $q_0 \approx 5 \times 10^{-3}$ and present universal density $\rho_0 \approx 2 \times 10^{-31}$ gm cm^{-3}.

11. The very low helium content recently observed in some stars could be the result of the original "big bang" if the universe contains degenerate neutrinos.

APPENDIX A

THERMODYNAMIC RELATIONS

The basic relation used in computing the thermodynamic properties of the photons and leptons is the distribution function for the number density of particles in the energy range dE,

$$n(E)\, dE = \frac{g}{2\pi^2 c^2 \hbar^3} \left[\exp\left(\frac{E+\Phi}{KT}\right) \pm 1 \right]^{-1} pE\, dE, \tag{A1}$$

where g is the number of spin states and the $+$ $(-)$ sign corresponds to Fermi-Dirac (Bose-Einstein) particles. For the photons, $\Phi = 0$. For the electrons and positrons, we also set $\Phi = 0$, which corresponds to the extreme non-degenerate approximation (Fowler and Hoyle 1964) of neglecting the difference between the number of electrons and positrons compared to their sum. Although this approximation breaks down when the positrons have annihilated, the electron density is then so low as to have no effect on the problem.

Besides being true for those particles in thermal equilibrium, equation (A1) also holds for those massless particles which "freeze out" during the expansion of the universe, i.e., the neutrinos, as may be easily proved. The temperature T_ν, which appears in the distribution function in this case, then satisfies the relation $T_\nu \propto R^{-1}$.

By use of equation (A1), the mass density of the photons is given by Stefan's law,

$$\rho_\gamma = ac^{-2}\, T^4 = 8.42 T_9{}^4 \text{ gm cm}^{-3}, \tag{A2}$$

while their pressure is

$$p_\gamma = \tfrac{1}{3}\rho_\gamma c^2 = 2.52 \times 10^{21}\, T_9{}^4 \text{ ergs cm}^{-3}. \tag{A3}$$

Similarly, in the case of the universe with no neutrino or antineutrino degeneracy, we obtain for each type of neutrino and antineutrino $\rho = \tfrac{7}{16} ac^{-2}\, T^4{}_\nu$, so that their total mass density is

$$\rho_\nu = \tfrac{7}{4} ac^{-2}\, T_\nu{}^4 = 14.73\, T_{9\nu}{}^4 \text{ gm cm}^{-3}, \tag{A4}$$

while their total pressure is

$$p_\nu = \tfrac{1}{3}\rho_\nu c^2 = 4.41 \times 10^{21}\, T_{9\nu}{}^4 \text{ ergs cm}^{-3}. \tag{A5}$$

At energies much higher than the electron rest mass, the Fermi-Dirac distribution must give the same results per degree of freedom for electrons and neutrinos, so that for $\rho_e = \rho(e^+) + \rho(e^-)$, we have

$$\rho_e = 2 \times \tfrac{7}{8}\rho_\gamma = \tfrac{7}{4}ac^{-2}\, T^4 \qquad (T_9 \gg 6), \tag{A6}$$

and

$$p_e = \tfrac{1}{3}\rho_e c^2 \qquad (T_9 \gg 6). \tag{A7}$$

Multiplying equation (A1) by E/c^2, expanding, and integrating gives (recalling $\Phi \approx 0$) the more general result

$$\rho_e = 15.56 T_9{}^4 \left[M(Z) - \tfrac{1}{16} M(2Z) + \ldots \right] \text{ gm cm}^{-3} , \tag{A8}$$

where

$$Z = \frac{m_e c^2}{KT} = \frac{5.93}{T_9} , \qquad M(Z) = \left[\bar{K}_3(Z) + \frac{Z^2}{24} \bar{K}_1(Z) \right] ,$$

$$\bar{K}_n(Z) = \frac{2}{(n-1)!} \left(\frac{Z}{2} \right)^n K_n(Z) \to 1 \qquad (Z \ll 1)$$

and $K_n(Z)$ is a hyperbolic Bessel function. We also have

$$p_e/c^2 = 5.19 T_9{}^4 \left[\bar{K}_2(Z) - \tfrac{1}{16} \bar{K}_2(2Z) + \ldots \right] \text{ gm cm}^{-3} . \tag{A9}$$

The error introduced by keeping only the first two terms in the series ≈ 1 per cent. As mentioned before, neglecting Φ is valid only as long as the total number of electrons and positrons, given by

$$n_e = 3.38 \times 10^{28} T_9{}^3 \left[\bar{K}_2(Z) - \tfrac{1}{8} \bar{K}_2(2Z) + \ldots \right] \text{ cm}^{-3} \tag{A10}$$

in this approximation, is much larger than the difference in number density of electrons and positrons, given by the total number density of positive charges

$$n_+ = \rho_b N_A \sum_i \frac{X_i}{A_i} Z_i \approx 6.02 \times 10^{23} h T_9{}^3 \sum_i \frac{X_i}{A_i} Z_i , \tag{A11}$$

where X_i, A_i, and Z_i are the mass fraction, mass number, and atomic number of the ith nucleus, while N_A is Avogadro's number.

The total density and pressure may be written as

$$\rho = \rho_1(T) + \rho_2(R) , \qquad p = p_1(T) + p_2(R) ,$$

where $\rho_1(T) = \rho_\gamma + \rho_e$, $\rho_2(R) = \rho_\nu + \rho_b$, $p_1(T) = p_\gamma + p_e$ and $p_2(R) = p_\nu$. The photon and electron density and pressure are best retained as functions of the temperature. The neutrino density and pressure may be considered functions of R alone because, as shown in § II, $T_\nu = T \propto R^{-1}$ before the neutrinos freeze out, while $T_\nu \propto R^{-1}$ after they freeze out. Using the fact that $\rho_b \propto R^{-3}$, the work-energy equation (7) can be put in the form

$$\frac{d}{dT} \left\{ \left[\rho_1(T) + \frac{p_1(T)}{c^2} \right] R^3 \right\} + \frac{4}{3} \frac{d}{dT} (\rho_\nu R^3) = R^3 \frac{d}{dT} \left[\frac{p_1(T)}{c^2} + \frac{\rho_\nu}{3} \right] . \tag{A12}$$

Since $\rho_\nu \propto R^{-4}$, the neutrino terms cancel, giving

$$\frac{dR}{dT} = \frac{-R}{3 \left[\rho_1(T) + p_1(T)/c^2 \right]} \frac{d\rho_1(T)}{dT} \xrightarrow[\substack{T_9 \gg 6 \\ T_9 \ll 6}]{} -\frac{R}{T} . \tag{A13}$$

The relation between photon temperature and time which is needed in order to use T as the independent variable in the integration of the rate equations is found by using the expansion rate (4),

$$\frac{dT}{dt} = \frac{dR/dt}{dR/dT} = \mp (24\pi G \rho)^{1/2} \left[\rho_1(T) + \frac{p_1(T)}{c^2} \right] \left[\frac{d\rho_1(T)}{dT} \right]^{-1} . \tag{A14}$$

At very high temperature ($T_9 \gtrsim 10$), where $\rho = \tfrac{9}{2}\rho_\gamma$, $\rho_1 = \tfrac{11}{4}\rho_\gamma$, and $T \propto R^{-1}$, this equation may be integrated with $T = \infty$ at $t = 0$ to give

$$T_9 = (12\pi G a c^{-2})^{1/4} t^{-1/2} = 10.4 \, t^{-1/2} , \tag{A15}$$

a relation which remains approximately true at lower temperatures, provided the radiation density is greater than the baryon density.

Using the facts that $T_\nu \to T$ at high temperatures and $T_\nu \propto R^{-1}$, it can be easily shown (Alpher *et al.* 1953) that the neutrino temperature is related to the photon temperature by the simple expression

$$\frac{T}{T_\nu} = \left[\frac{(11/4)(\rho_\gamma + p_\gamma/c^2)}{\rho_1(T) + p_1(T)/c^2} \right]^{1/3} \xrightarrow[T_9 \ll 6]{} 1.40. \tag{A16}$$

The factor $\frac{11}{4} = 2.75$ represents the additional degrees of freedom converted into the radiation field when the pairs annihilate.

Details of much of the above material are provided by Alpher *et al.* (1953) and Fowler and Hoyle (1964).

APPENDIX B

COMPUTATION OF REACTION RATES

The reaction rates are essentially defined by the structure of the rate equation (16). We may also write the rate equations in the form

$$\frac{dX_i}{dt} = F_i(X_j,T) - X_i G_i(X_k,T), \tag{A17}$$

where, in the equation for $X_i = X(\mathrm{He}^3)$, for instance,

$$
\begin{aligned}
F(\mathrm{He}^3) = {} & \tfrac{3}{2}X(p)X(\mathrm{D})[p\mathrm{D}] + \tfrac{3}{8}X(\mathrm{D})^2 [\mathrm{DD}]_n + X(p)X(\mathrm{T})[p\mathrm{T}]_n \\
& + \tfrac{3}{4}X(\mathrm{He}^4)\{\lambda_\gamma (\mathrm{He}^4)_n + X(p)[p\mathrm{He}^4] + X(p)^2 [pp\mathrm{He}^4] \\
& + X(p)X(n)[pn\mathrm{He}^4] + \tfrac{1}{2}X(\mathrm{D})[\mathrm{DHe}^4]\} + \tfrac{3}{7}X(\mathrm{Be}^7)\lambda_\gamma (\mathrm{Be}^7) \\
G(\mathrm{He}^3) = {} & \lambda_\gamma (\mathrm{He}^3) + X(n)([n\mathrm{He}^3]_p + [n\mathrm{He}^3]_\mathrm{D} + [n\mathrm{He}^3]_\gamma) \\
& + \tfrac{1}{2}X(\mathrm{D})[\mathrm{DHe}^3] + \tfrac{1}{3}X(\mathrm{He}^3)[\mathrm{He}^3\mathrm{He}^3] + \tfrac{1}{3}X(\mathrm{T})([\mathrm{He}^3\mathrm{T}]_{pn} \\
& + [\mathrm{He}^3\mathrm{T}]_\mathrm{D}) + \tfrac{1}{4}X(\mathrm{He}^4)[\mathrm{He}^3\mathrm{He}^4].
\end{aligned}
$$

The subscripts on some of the rates are to distinguish between various end products.

The reaction rates $\lambda_k(j)$ corresponding to the interaction of a lepton or photon k with a nucleus j, are given by

$$\lambda_k(j) = \int_0^\infty n_k(E,T,\Phi) \sigma(E) v(E) dE, \tag{A18}$$

where n_k is the distribution function (A1) appropriate to particle k, $\sigma(E)$ is the cross-section, and v and E are the velocity and energy of the lepton or photon in the center-of-momentum frame. For a free decay, $\lambda_\beta(j)$ is just the inverse mean lifetime.

The calculation of the n-p weak reactions (1)–(3) in Table 2(a) was done on the basis of the current theory of β-decay (Bjorken and Drell 1964), using the invariant amplitude

$$\mathfrak{M} = \frac{G}{\sqrt{2}}[\bar{u}_p \gamma_\mu(1 - a\gamma_5)u_n][\bar{u}_e \gamma^\mu(1 - \gamma_5)v_{\bar{\nu}}]. \tag{A19}$$

For the two-particle processes (1) and (2) in Table 2(a), we find

$$\sigma v = \frac{2\pi^2}{g\tau}\left(\frac{\hbar}{m_e c}\right)^3 \left(\frac{pE}{m_e^2 c^3}\right) F, \tag{A20}$$

where g is the number of spin states for the incident lepton, F is the fraction of phase space available to the emerging lepton, p and E its momentum and energy, while τ is determined from the lifetime of the neutron. Using the appropriate distribution functions, we obtain

$$\lambda_\nu(n) = \frac{1}{\tau} \int_q^\infty \frac{(\epsilon - q)^2 e^{\epsilon Z}(\epsilon^2 - 1)^{1/2}\epsilon d\epsilon}{(1 + e^{\epsilon Z})[1 + e^{(\epsilon-q)Z_\nu - \phi_\nu}]}, \tag{A21}$$

$$\lambda_{e^+}(n) = \frac{1}{\tau} \int_1^\infty \frac{(\epsilon + q)^2 e^{(\epsilon+q)Z_\nu + \phi_\nu}(\epsilon^2 - 1)^{1/2}\epsilon d\epsilon}{(1 + e^{\epsilon Z})[1 + e^{(\epsilon+q)Z_\nu + \phi_\nu}]}, \tag{A22}$$

$$\lambda_{e^-}(p) = \frac{1}{\tau} \int_q^\infty \frac{(\epsilon - q)^2 e^{(\epsilon-q)Z_\nu - \phi_\nu}(\epsilon^2 - 1)^{1/2}\epsilon d\epsilon}{(1 + e^{\epsilon Z})[1 + e^{(\epsilon-q)Z_\nu - \phi_\nu}]}, \tag{A23}$$

$$\lambda_{\bar\nu}(p) = \frac{1}{\tau} \int_1^\infty \frac{(\epsilon + q)^2 e^{\epsilon Z}(\epsilon^2 - 1)^{1/2}\epsilon d\epsilon}{(1 + e^{\epsilon Z})[1 + e^{(\epsilon+q)Z_\nu + \phi_\nu}]}, \tag{A24}$$

where $q = (m_n - m_p)/m_e = 2.53$, $Z = m_e c^2/kT$, $Z_\nu = m_e c^2/kT_\nu$, and $\phi_\nu = \Phi_\nu/kT_\nu$.

For the neutron decay, one obtains in a similar manner,

$$\lambda(n) = \frac{1}{\tau} \int_1^q \frac{(\epsilon - q)^2 e^{\epsilon Z} e^{(q-\epsilon)Z_\nu + \phi_\nu}(\epsilon^2 - 1)^{1/2}\epsilon d\epsilon}{(1 + e^{\epsilon Z})[1 + e^{(q-\epsilon)Z_\nu + \phi_\nu}]}. \tag{A25}$$

Evaluating the integral for $T = T_\nu \to 0$ allows one to determine τ in terms of the measured half-life $t_{1/2}$ of the neutron:

$$\tau = \frac{I t_{1/2}}{\ln 2} = 1700, \tag{A26}$$

where $I = 1.67$ is the value of the integral, while $t_{1/2} = 704$ sec. The reverse reaction rate can be found by invoking statistical balance and comparing phase space factors. It is thus

$$\lambda_{e^-\bar\nu}(p) = \frac{1}{\tau} \int_1^q \frac{(\epsilon - q)^2(\epsilon^2 - 1)^{1/2}\epsilon d\epsilon}{(1 + e^{\epsilon Z})[1 + e^{(q-\epsilon)Z_\nu + \phi_\nu}]}. \tag{A27}$$

In fact, the other reverse rates could also have been determined in this manner.

By combining both the direct and inverse rates, we obtain the total rates for destroying neutrons and protons given in Table 2(a). We obtain the rates for these processes within a massive star by simply taking the limit $T_\nu \to 0$ ($Z_\nu \to \infty$), $\phi_\nu \to 0$.

The quantities $\langle \sigma v \rangle_{jk}$, corresponding to the interaction of two nuclei, are given by

$$\langle \sigma v \rangle_{jk} = \int_0^\infty f(v, T)\sigma(v) v dv. \tag{A28}$$

Here $f(v,T)$ is the Boltzmann distribution function for the nuclei of temperature T and v their relative velocity. A useful expression for the reaction rate is

$$[jk] = \rho_b N_A \langle \sigma v \rangle_{jk} = 3.73 \times 10^{10} \rho_b A^{-1/2} T_9^{-3/2} \int \sigma E e^{-11.6 E/T_9} dE, \tag{A29}$$

where A is the reduced mass number, σ is expressed in barns, and the center-of-momentum energy E is expressed in MeV.

For measured non-resonant reactions between nuclei, the expression derived by Bahcall (1966) was used. A convenient form is

$$[jk] = 7.83 \times 10^6 \rho_b A^{-1/3} (Z_j Z_k)^{1/3} T_9^{-2/3} e^{-\tau} S_{\text{eff}}, \tag{A30}$$

where $\tau = 4.249\ (Z_j^2 Z_k^2\ A\ T_9^{-1})^{1/3}$, and

$$S_{\text{eff}} = S(0)\ [1 + 0.09807\ (Z_j Z_k)^{-2/3}\ A^{-1/3}\ T_9^{1/3}] + S'(0)\ [122.04\ (Z_j Z_k)^{2/3}\ A^{1/3}\ T_9^{2/3}$$

$$+ 83.776\ T_9] + S''(0)\ [7.447 \times 10^3\ (Z_j Z_k)^{4/3}\ A^{2/3}\ T_9^{4/3}$$

$$+ 1.300 \times 10^4\ (Z_j Z_k)^{2/3}\ A^{1/3}\ T_9^{5/3}]$$

in barns-keV. The slowly varying quantity $S(E)$ is defined by the relation (Burbidge et al. 1957)

$$\sigma = \frac{S(E)}{E} \exp\left[-2\pi a Z_j Z_k \left(\frac{Mc^2}{2}\right)^{1/2} E^{-1/2} \right], \qquad \text{(A31)}$$

where M is the reduced mass of the colliding nuclei, Z_j and Z_k are their charges, while the cross-section factor S and its derivatives at zero energy are expressed in barns-keV, barns, and barns-keV^{-1}, respectively. The adopted values for these quantities will be found in Fowler et al. (1967). It is important to note that equation (A30) is only valid under the condition $\tau > 1$. We find this condition to hold in all cases considered. Furthermore we find, in general, that the term in $S''(0)$ should be omitted if the contribution (A32) (below) of a low-lying resonance is included.

For computing other reaction rates, the appropriate formulae appearing in Appendix C of Fowler and Hoyle (1964) were used. In the case that individual resonances in the compound nucleus are narrower than the thermal energy, and width and spin measurements or estimations are available for each, we obtain

$$\log [jk] = 11.19 + \log \rho_b - \tfrac{3}{2} \log A T_9$$

$$+ \log \sum_r (\omega \Gamma_1 \Gamma_2 / \Gamma)_r \exp(-11.6\ E_r / T_9), \qquad \text{(A32)}$$

where the widths of the incoming channel Γ_1, outgoing channel Γ_2, total width Γ, and resonance energy E_r are in MeV, and where $\omega = (2J + 1)/(2J_j + 1)(2J_k + 1)$ is the statistical factor applying to the formation of the state with spin J from the initial nuclei with spins J_j and J_k.

In estimating many of the reaction rates involving the heavier elements, we have used the fact that, at sufficiently high excitation, compound nuclei exhibit overlapping resonances, so that continuum cross-sections may be used. The energy dependence is then dominated mainly by optical model and barrier penetration factors. For most particle-particle reactions, such as (He^4,p) and (p,He^4), where $\Gamma_2 \approx \Gamma$, we have used equation (C61) of Fowler and Hoyle (1964) to obtain

$$\log [jk] \approx 8.71 + \log \rho_b + \tfrac{4}{3} \log Z_j Z_k - \tfrac{5}{6} \log A + 0.457\ (A Z_j Z_k R_f)^{1/2}$$

$$- \tfrac{2}{3} \log T_9 - 1.845\ (Z_j^2 Z_k^2\ A/T_9)^{1/3}. \qquad \text{(A33)}$$

The interaction radius in fermis, $R_f \approx 1.07\ (A_0)^{1/3} + a_f$, with A_0 equal to the mass number of the heavy nucleus, and a_f equal to 2.17 for an incoming p, 3.51 for D, 3.10 for T, 3.27 for He^3, and 3.01 for He^4.

For many of the unknown particle-γ reactions (p,γ) and (He^4,γ), in which $\Gamma_1 \approx \Gamma$, we have used equation (C61') of Fowler and Hoyle (1964) to obtain

$$\log [jk] \approx 8.48 + \log \rho_b + 2 \log R_f + \tfrac{1}{2} \log T_9/A + \log \langle \Gamma_\gamma/D \rangle_{\ell_e}$$

$$- 5.04\ E_0^*/T_9. \qquad \text{(A34)}$$

An analysis of empirical data for the ratio of γ-width to level spacing yielded

$$\log \left\langle \frac{\Gamma_\gamma}{D} \right\rangle_{\ell e} = -6.70 - 2 \log A_c + 0.29 (A_c B')^{1/2} + \frac{3.90}{(A_c B')^{1/2}}.$$

Here A_c is the mass number of the compound nucleus, the effective Coulomb barrier height $E_0^* = 0.4 Z_j Z_k / R_f$ MeV, and $B' = Q + E_0^* - \Delta$, where Q is the energy release (in MeV) of the reaction, and $\Delta = 0$, 1.5 and 3.0 MeV for odd Z–odd N, odd A, and even Z–even N compound nuclei, respectively. We have made the substitution $T_9^* = 5.93 (Z_j Z_k / A R_f^3)^{1/2}$.

If the reaction rate corresponding to the process $0 + 1 \rightarrow 2 + 3$ is known, then the rate for the inverse reaction can be obtained by employing statistical equilibrium, giving

$$[23] = \frac{g_0 g_1}{g_2 g_3} \left(\frac{A_0 A_1}{A_2 A_3} \right)^{3/2} \exp \left(-\frac{11.6 Q}{T_9} \right) [01] \left(\frac{1 + \delta_{23}}{1 + \delta_{01}} \right), \tag{A35}$$

where $g_i = 2 J_i + 1$ is the number of spin states of nucleus i. Similarly, if the rate for $0 + 1 \rightarrow 2 + \gamma$ is known, the inverse rate is given by

$$\lambda_\gamma(2) = 1.0 \times 10^{10} \frac{g_0 g_1}{g_2} \left(\frac{A_0 A_1}{A_2} \right)^{3/2} T_9^{3/2} \exp \left(-\frac{11.6 Q}{T_9} \right) \frac{[01]}{\rho_b} \left(\frac{1}{1 + \delta_{01}} \right). \tag{A36}$$

REFERENCES

Alpher, R. A., Bethe, H. A., and Gamow, G. 1948, *Phys. Rev.*, **73**, 803.
Alpher, R. A., Follin, J. W., and Herman, R. C. 1953, *Phys. Rev.*, **92**, 1347.
Bahcall, J. N. 1966, *Ap. J.*, **143**, 259.
Bardeen, J. M. 1965, unpublished Ph.D. thesis, California Institute of Technology.
Bardeen, J. M., and Anand, S. P. S. 1966 (to be published).
Bjorken, J. D., and Drell, S. D. 1964, *Relativistic Quantum Mechanics* (New York: McGraw-Hill Book Co.).
Burbidge, E. M , Burbidge, G. R., Fowler, W. A., and Hoyle, F. 1957, *Rev. Mod. Phys.*, **29**, 547.
Chandrasekhar, S. 1964, *Ap. J.*, **140**, 417.
Christy, R. F. 1966, *Ap. J.*, **144**, 108.
Cowsik, R., Pal, V., and Tandon, S. V. 1964, *Phys. Letters*, **13**, 265.
Dicke, R. H., Peebles, P. J. E., Roll, P. G., and Wilkinson, D. T. 1965, *Ap. J.*, **142**, 414.
Faulkner, J. 1966, *Ap. J.*, **144**, 978.
Felten, J. 1966, *Ap. J.*, **144**, 241.
Fermi, E., and Turkevich, A. 1950, quoted in R. A. Alpher and R. C. Herman, 1950, *Rev. Mod. Phys* , **22**, 153.
Field, G. B., and Hitchcock, J. C. 1966, *Phys. Rev. Letters*, **16**, 817.
Fowler, W. A. 1964, *Rev. Mod. Phys.*, **36**, 545, 1140E.
———. 1966, *Ap. J.*, **144**, 180.
Fowler, W. A., Caughlan, G. R., and Zimmerman, B. 1967 (to be published)
Fowler, W. A., Greenstein, J. L., and Hoyle, F. 1962, *Geophys. J. R.A.S.*, **6**, 148.
Fowler, W. A., and Hoyle, F. 1960, *Ann. Phys.*, **10**, 280.
———. 1964, *Ap. J. Suppl. No. 91*, **9**, 201.
Greenstein, J. L. 1966, *Ap. J.*, **144**, 496.
Hayashi, C. 1950, *Progr. Theoret. Phys.*, **5**, 224.
Hayashi, C., Hōshi, R., and Sugimoto, D. 1962, *Progr. Theoret. Phys. Suppl. No. 22*, p. 1.
Hayashi, C., and Nishida, M. 1956, *Progr. Theoret. Phys.*, **16**, 613.
Herbig, G. 1964, *Ap. J.*, **140**, 702.
Hoyle, F., and Tayler, R. J. 1964, *Nature*, **203**, 1108.
Iben, I., Jr. 1965a, *Ap. J.*, **141**, 993.
———. 1965b, *ibid.*, **142**, 1447.
———. 1966, *ibid.*, **143**, 483.
Kaufman, M. 1965, *Nature*, **207**, 736.
Layzer, D. 1966, *Nature*, **211**, 576.
Merchant, A. E. 1966, *Ap. J.*, **143**, 336.
Merrill, P. W. 1952, *Science*, **115**, 484.
Oort, J. H. 1958, *La Structure et l'Évolution de l'Univers* (Brussels: R. Stoops)

Pagel, B. 1965, *Nature*, **206**, 282.
Peebles, P. J. E. 1966a, *Phys. Rev. Letters*, **16**, 410.
————. 1966b, *Ap. J.*, **146**, 542.
Penzias, A. A., and Wilson, R. W. 1965, *Ap. J.*, **142**, 419.
Roll, P. G., and Wilkinson, D. T. 1966, *Phys. Rev. Letters*, **16**, 405.
Salpeter, E. E. 1959, *Ap. J.*, **129**, 608.
Sandage, A. 1961, *Ap. J.*, **133**, 355.
————. 1962, in *Problems of Extra-Galactic Research*, ed. G. C. McVittie (New York: Macmillan Co).
Sargent, W. L. W., and Searle, L. 1966, *Ap. J.*, **145**, 652.
Schmidt, M. 1959, *Ap. J.*, **129**, 243.
Signer, P., and Suess, H. 1964, *Earth Science and Meteoritics* (Amsterdam: North-Holland Publishing Co.).
Spanur, J. 1966 *Zs f. Phys* , **191**, 24.
Thaddeus, P., and Clauser, J. F. 1966, *Phys. Rev. Letters*, **16**, 819.
Urey, H. 1952, *The Planets* (London: Oxford University Press), p. 148; see also Kokubu, N., Mayeda, T., and Urey, H. C. 1961, *Geochim. et Cosmochim. Acta*, **21**, 247.
Wright, J. P. 1964, *Phys. Rev.*, **136**, B288.
Zel'dovich, Ya. B. 1964, *Soviet J. Atomic Energy*, **14**, 83.